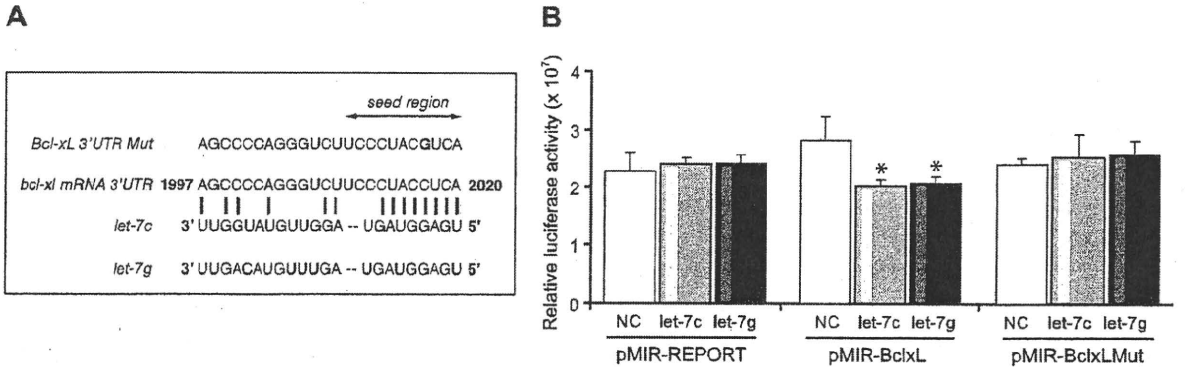

Fig. 3. Sequence-specific suppression of *bcl-xl* gene expression by *let-7c* or *let-7g* miRNAs. (A) The putative target site of *bcl-xl* mRNA 3′UTR determined by computational predictions. The target sequence was cloned into pMIR-REPORT vector (pMIR-Bcl-xL-3′UTR). pMIR-Bcl-xL-3′UTR mutant was also generated with a single mutation (indicated by a bold character) in the target site. (B) Each of these constructs was transfected into Huh7 cells together with *let-7c*, *let-7g* or negative control miRNA (NC). At 24 h after transfection, the activity of firefly luciferase was measured and normalised to β-galactosidase expression levels ($n = 3$). $^*p < 0.05$.

induced by *let-7c* or *let-7g*, which strongly suggests a direct inhibitory effect of *let-7* on Bcl-xL expression (Fig. 3B).

Downregulation of let-7c miRNA in human HCC tissues overexpressing Bcl-xL but not bcl-xl mRNA

To investigate the relationship between *let-7* expression levels and Bcl-xL protein levels in human HCC samples, we used 22 pairs of surgically resected human HCC tissue samples and adjacent non-tumour tissue samples with highly preserved RNA. Compared to the non-tumour counterparts, *bcl-xl* mRNA was found to be over-expressed in HCC tissue samples in only two cases; Bcl-xL was also over-expressed at the protein level in these cases. To assess the significance of *let-7* in post-transcriptional regulation of Bcl-xL *in vivo*, we selected 20 pairs of HCC tissue samples that did not over-express *bcl-xl* mRNA. When these samples were divided into two groups according to relative *let-7c* expression levels, the relative expression of Bcl-xL protein was significantly higher in the *let-7c* low expression group than in the *let-7c* high expression group (Fig. 4). By contrast, there was no significant difference in *bcl-xl* mRNA expression between the two groups. We also examined the relationship between relative *let-7g* expression and Bcl-xL expression. The *let-7g* low expression group tended to over-express Bcl-xL protein compared to the *let-7g* high expression group, although the difference did not reach statistical significance (data not shown). These results are consistent with the hypothesis that *let-7* miRNAs negatively regulate Bcl-xL expression independent of transcriptional regulation.

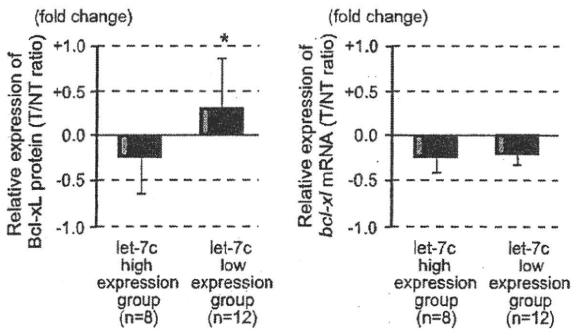

Fig. 4. Expression of Bcl-xL, *bcl-xl* mRNA and *let-7* miRNAs in human HCC tissue. Relationship between *let-7* and Bcl-xL expression in human HCC tissue samples. HCC tissue samples that did not show transcriptional upregulation of *bcl-xl* mRNA were divided into two groups according to relative *let-7c* expression levels with the threshold set at a 0.4-fold change in the tumour to non-tumour (T/NT) ratio. Relative expression of Bcl-xL protein and *bcl-xl* mRNA was calculated as the optical densities of the Bcl-xL blots normalised with the β-actin blots and those of real time RT-PCR assays, respectively, and are shown as the ratio of expression in the tumour to non-tumour expression in $\log_{10}$ scale. $^*p < 0.05$.

let-7c miRNA sensitises human Huh7 cells to sorafenib, which downregulates Mcl-1 expression

To investigate the effect of *let-7* in the resistance of hepatoma cells to apoptosis, we transfected Huh7 hepatoma cells with *let-7c* miRNAs and then subjected them to apoptosis analysis and a cell viability assay. There was no significant difference in caspase-3/7 activation or cell viability between *let-7c* miRNA-transfected Huh7 cells and control miRNA-transfected Huh7 cells (represented by the DMSO-treated group of Fig. 5A and B). These results are in agreement with our previous finding that anti-sense oligonucleotide-mediated knockdown of Bcl-xL sensitised hepatoma cells to apoptotic stimuli, such as serum starvation and *p53* activation, but did not induce apoptosis by itself [13]. Next, we exposed miRNA-transfected Huh7 cells to staurosporine, which is a well-established apoptosis inducer. Staurosporine treatment induced apoptosis, as determined by caspase-3/7 activation and decreased the viability of Huh7 cells by itself, but *let-7c* miRNA-transfected Huh7 cells were more susceptible to staurosporine treatment than control miRNA-transfected cells. *let-7c* miRNA-transfected Huh7 cells showed a significant decrease in cell viability, even upon exposure to low-dose of staurosporine at which control miRNA-transfected Huh7 did not show a significant difference in cell viability (Fig. 5B). In addition, the activation of caspase-3/7 was more intense in *let-7c* miRNA-transfected Huh7 cells than in control miRNA-transfected Huh7 cells (Fig. 5A). Thus, suppression of *let-7* expression leading to over-expression of Bcl-xL, may be a mechanism by which hepatoma cells resist apoptotic stimuli. While normal hepatocytes were more sensitive to staurosporine than hepatoma cells, transfection of *let-7* miRNA did not affect sensitivity to staurosporine

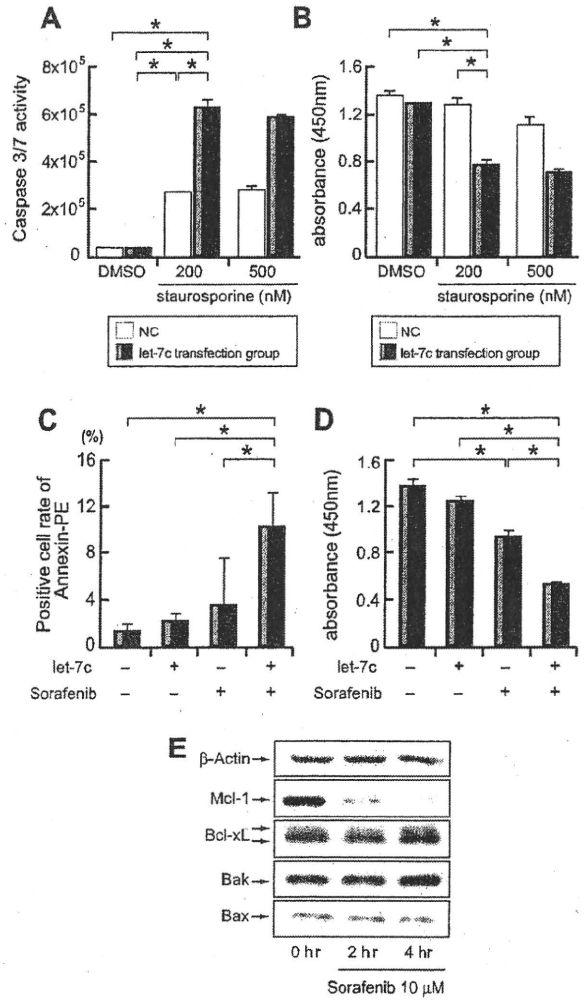

Fig. 5. Introduction of *let-7* miRNAs sensitises hepatoma cells to apoptotic stimuli. (A and B) Response to staurosporine treatment. Huh7 cells were transfected with *let-7c* (grey bars) or control miRNA (white bars) for 48 h and then further treated with staurosporine or DMSO alone for 12 h. The activities of caspase-3 and -7 were determined by luminescent substrate assays for caspase-3 and -7 ($n = 4$) (A). Cell viability was determined by the WST assay ($n = 4$) (B). *$p < 0.05$. (C and D) Response to sorafenib treatment. Huh7 cells were transfected with *let-7c* or control miRNA for 48 h and then further treated with sorafenib (5 μM) or DMSO alone for 48 h (C) or 72 h (D) 7-AAD negative cells were gated and the positive cell rate for annexin V-PE was determined ($n = 4$) (C). Cell viability was determined by the WST assay ($n = 4$) (D). *$p < 0.05$. E. Western blot analysis for Bcl-2 family proteins in lysates of Huh7 cells treated with sorafenib.

in normal hepatocytes (Suppl. Fig. 2), which is in agreement with the modest decline of Bcl-xL expression described earlier.

To examine the impact of *let-7* family miRNAs as a therapeutic tool, we investigated the effect of *let-7* miRNAs on apoptosis resistance to sorafenib, a recently approved anti-cancer drug for HCC. It has been reported that sorafenib was capable of downregulating Mcl-1 expression in tumour cells [24], and HCC has been reported to over-express Mcl-1, which is another anti-apoptotic Bcl-2 protein capable of conferring resistance to apoptosis [24–27]. In agreement with these findings, sorafenib treatment clearly downregulated Mcl-1 expression in hepatoma cells, but did not affect Bcl-xL expression (Fig. 5E). In contrast, sorafenib treatment did not affect Mcl-1 expression in normal hepatocytes (Suppl. Fig. 3). We hypothesised that *let-7* miRNA targeting Bcl-xL may induce apoptosis of hepatoma cells in cooperation with sorafenib. Apoptosis determined by Annexin V staining did not increase in *let-7c* miRNA-treated Huh7 cells compared to control miRNA-treated cells (represented by the DMSO-treated group in Fig. 5C). Sorafenib treatment of Huh7 cells led to a slight increase in the annexin V-positive cell rate, although the difference did not reach statistical significance levels under our experimental conditions (Fig. 5C). Of importance is the finding that sorafenib-induced apoptosis was markedly enhanced in *let-7c* miRNA-transfected cells. In addition, sorafenib treatment significantly reduced the viability of Huh7 cells and this decrease was markedly enhanced in cells transfected with *let-7c* miRNA (Fig. 5D). This finding implies that *let-7* miRNA transfection potentiates sorafenib-induced apoptosis and toxicity in hepatoma cells.

Discussion

Anti-apoptotic members of the Bcl-2 family, which consists of five members, Bcl-2, Bcl-xL, Mcl-1, Bcl-w, and Bfl-1, are critically involved in the mitochondrial pathway of apoptosis [28]. Cancer cells frequently over-express one or more members of this family to acquire a survival advantage [29]. These proteins are over-expressed in a variety of ways, including genetic translocation, particularly in the case of Bcl-2, and transcriptional regulation. Unlike the case of the *bcl-2* gene, mutations or amplification of the *bcl-x* gene have not been demonstrated in tumour cells. With regard to miRNA regulation, previous research clearly demonstrated that Bcl-2 is a direct target of *miR-15* and *miR-16*. The expression levels of *miR-15* and *miR-16* inversely correlate with Bcl-2 expression in chronic lymphocytic leukaemia [30]. More recently, Mcl-1 was reported to be suppressed by *miR-29* [31]. Our present study is the first demonstration of miRNA-mediated regulation of Bcl-xL expression. Since Bcl-xL is over-expressed not only in HCC but also in other tumours, the present findings may shed light on the mechanisms of Bcl-xL over-expression in other malignancies.

While more than 500 human miRNAs have been identified, *let-7* is a prototype of human miRNA and was first identified in 2001 [32]. *let-7* miRNAs are downregulated in several malignancies. A highly characterised example is non-small cell lung cancer in which downregulation of *let-7* miRNAs is well correlated with poor prognosis in patients [33]. In HCC, some reports showed downregulation of *let-7*, while others did not [7]. In the present study, *let-7c* miRNA was under-expressed at less than 40% of the normal level in approximately half of the HCC tissues. Further study is needed to determine the clinical significance of *let-7* miRNA in HCC. Several target genes have been identified for *let-7* miRNA, including Ras [34], Myc [35], HMGA2 [36], CDC25A, and CDK6 [37]. The major function of this miRNA is to promote cell proliferation. Since these proteins could act as oncogenes in tumour cells, *let-7* miRNA is believed to serve as a tumour suppressor [38]. In the present study, we have demonstrated that *bcl-xl* is a direct target for *let-7* miRNA, implying that this well-known tumour suppressor miRNA directly regulates apoptosis, another important process in malignancy.

Sorafenib is a recent FDA-approved anti-cancer drug for HCC [21]. It functions as a multi-kinase inhibitor and can induce

apoptosis at least in part by downregulating Mcl-1 in tumour cells [24]. Like Bcl-xL, several reports have identified Mcl-1 as being over-expressed in some HCCs [25–27]. Since Bcl-xL and Mcl-1 share a similar structure and functions, we reasoned that downregulation of both proteins would efficiently kill hepatoma cells. To verify this hypothesis, we treated hepatoma cells with sorafenib and *let-7* miRNA. As expected, sorafenib treatment downregulated Mcl-1 expression as early as 2 h post-treatment; however, it did not efficiently induce apoptosis. Transfection of *let-7* miRNA itself was not capable of inducing apoptosis of hepatoma cells despite a clear reduction in Bcl-xL expression. Importantly, *let-7* miRNA substantially increased sensitivity to sorafenib. Since both *let-7* miRNA and sorafenib may have pleiotropic effects on gene expression and cellular processes, downregulation of Bcl-xL and Mcl-1 may not be a single mechanism for killing hepatoma cells. However, our study revealed that Bcl-xL-targeting miRNA, *let-7*, controls resistance of hepatoma cells to this novel class of anti-HCC drug.

In conclusion, we have demonstrated that *let-7* miRNA negatively regulates Bcl-xL expression in HCCs. Reconstitution of *let-7* miRNA may reduce apoptosis resistance to anti-cancer drugs targeting Mcl-1 in HCC. Further study is needed to examine the significance of *let-7* miRNA expression for predicting responses to sorafenib therapy in patients with HCC.

Financial support

This work was partly supported by a Grant-in-Aid for Scientific Research from the Ministry of Education, Culture, Sports, Science and Technology, Japan (to T. Tak).

Disclosures

All authors have nothing to disclose.

Conflicts of interest

All authors have no conflicts of interest.

Acknowledgements

We thank Bayer HealthCare Pharmaceuticals Inc. (Wayne, NJ) for providing sorafenib.

Appendix A. Supplementary data

Supplementary data associated with this article can be found, in the online version, at doi:10.1016/j.jhep.2009.12.024.

References

[1] Filipowicz W, Bhattacharyya SN, Sonenberg N. Mechanisms of post-transcriptional regulation by microRNAs: are the answers in sight? Nat Rev Genet 2008;9:102–114.
[2] Esquela-Kerscher A, Slack FJ. Oncomirs – microRNAs with a role in cancer. Nat Rev Cancer 2006;6:259–269.
[3] Zhang B, Pan X, Cobb GP, Anderson TA. MicroRNAs as oncogenes and tumor suppressors. Dev Biol 2007;302:1–12.
[4] Murakami Y, Yasuda T, Saigo K, Urashima T, Toyoda H, Okanoue T, et al. Comprehensive analysis of microRNA expression patterns in hepatocellular carcinoma and non-tumorous tissues. Oncogene 2006;25:2537–2545.
[5] Varnholt H, Drebber U, Schulze F, Wedemeyer I, Schirmacher P, Dienes HP, et al. MicroRNA gene expression profile of hepatitis C virus-associated hepatocellular carcinoma. Hepatology 2008;47:1223–1232.
[6] Wong QW, Lung RW, Law PT, Lai PB, Chan KY, To KF, et al. MicroRNA-223 is commonly repressed in hepatocellular carcinoma and potentiates expression of Stathmin1. Gastroenterology 2008;135:257–269.
[7] Gramantieri L, Ferracin M, Fornari F, Veronese A, Sabbioni S, Liu CG, et al. Cyclin G1 is a target of miR-122a, a microRNA frequently downregulated in human hepatocellular carcinoma. Cancer Res 2007;67:6092–6099.
[8] Meng F, Henson R, Wehbe-Janek H, Ghoshal K, Jacob ST, Patel T. MicroRNA-21 regulates expression of the PTEN tumor suppressor gene in human hepatocellular cancer. Gastroenterology 2007;133:647–658.
[9] Fornari F, Gramantieri L, Ferracin M, Veronese A, Sabbioni S, Calin GA, et al. MiR-221 controls CDKN1C/p57 and CDKN1B/p27 expression in human hepatocellular carcinoma. Oncogene 2008;27:5651–5661.
[10] Wang Y, Lee AT, Ma JZ, Wang J, Ren J, Yang Y, et al. Profiling microRNA expression in hepatocellular carcinoma reveals microRNA-224 up-regulation and apoptosis inhibitor-5 as a microRNA-224-specific target. J Biol Chem 2008;283:13205–13215.
[11] Budhu A, Jia HL, Forgues M, Liu CG, Goldstein D, Lam A, et al. Identification of metastasis-related microRNAs in hepatocellular carcinoma. Hepatology 2008;47:897–907.
[12] Ladeiro Y, Couchy G, Balabaud C, Bioulac-Sage P, Pelletier L, Rebouissou S, et al. MicroRNA profiling in hepatocellular tumors is associated with clinical features and oncogene/tumor suppressor gene mutations. Hepatology 2008;47:1955–1963.
[13] Takehara T, Liu X, Fujimoto J, Friedman SL, Takahashi H. Expression and role of Bcl-xL in human hepatocellular carcinomas. Hepatology 2001;34:55–61.
[14] Watanabe J, Kushihata F, Honda K, Sugita A, Tateishi N, Mominoki K, et al. Prognostic significance of Bcl-xL in human hepatocellular carcinoma. Surgery 2004;135:604–612.
[15] Ding ZB, Shi YH, Zhou J, Qiu SJ, Xu Y, Dai Z, et al. Association of autophagy defect with a malignant phenotype and poor prognosis of hepatocellular carcinoma. Cancer Res 2008;68:9167–9175.
[16] Chiao PJ, Na R, Niu J, Sclabas GM, Dong Q, Curley SA. Role of Rel/NF-kappaB transcription factors in apoptosis of human hepatocellular carcinoma cells. Cancer 2002;95:1696–1705.
[17] Selvendiran K, Koga H, Ueno T, Yoshida T, Maeyama M, Torimura T, et al. Luteolin promotes degradation in signal transducer and activator of transcription 3 in human hepatoma cells: an implication for the antitumor potential of flavonoids. Cancer Res 2006;66:4826–4834.
[18] Otsuka M, Kato N, Taniguchi H, Yoshida H, Goto T, Shiratori Y, et al. Hepatitis C virus core protein inhibits apoptosis via enhanced Bcl-xL expression. Virology 2002;296:84–93.
[19] Sarcar B, Ghosh AK, Steele R, Ray R, Ray RB. Hepatitis C virus NS5A mediated STAT3 activation requires co-operation of Jak1 kinase. Virology 2004;322:51–60.
[20] Pasquinelli AE, Reinhart BJ, Slack F, Martindale MQ, Kuroda MI, Maller B, et al. Conservation of the sequence and temporal expression of let-7 heterochronic regulatory RNA. Nature 2000;408:86–89.
[21] Llovet JM, Bruix J. Molecular targeted therapies in hepatocellular carcinoma. Hepatology 2008;48:1312–1327.
[22] Takehara T, Tatsumi T, Suzuki T, Rucker 3rd EB, Hennighausen L, Jinushi M, et al. Hepatocyte-specific disruption of Bcl-xL leads to continuous hepatocyte apoptosis and liver fibrotic responses. Gastroenterology 2004;127:1189–1197.
[23] Takehara T, Takahashi H. Suppression of Bcl-xL deamidation in human hepatocellular carcinomas. Cancer Res 2003;63:3054–3057.
[24] Rahmani M, Davis EM, Bauer C, Dent P, Grant S. Apoptosis induced by the kinase inhibitor BAY 43-9006 in human leukemia cells involves down-regulation of Mcl-1 through inhibition of translation. J Biol Chem 2005;280:35217–35227.
[25] Sieghart W, Losert D, Strommer S, Cejka D, Schmid K, Rasoul-Rockenschaub S, et al. Mcl-1 overexpression in hepatocellular carcinoma: a potential target for antisense therapy. J Hepatol 2006;44:151–157.
[26] Fleischer B, Schulze-Bergkamen H, Schuchmann M, Weber A, Biesterfeld S, Müller M, et al. Mcl-1 is an anti-apoptotic factor for human hepatocellular carcinoma. Int J Oncol 2006;28:25–32.
[27] Schulze-Bergkamen H, Fleischer B, Schuchmann M, Weber A, Weinmann A, Krammer PH, et al. Suppression of Mcl-1 via RNA interference sensitizes human hepatocellular carcinoma cells towards apoptosis induction. BMC Cancer 2006;6:232.
[28] Youle RJ, Strasser A. The BCL-2 protein family: opposing activities that mediate cell death. Nat Rev Mol Cell Biol 2008;9:47–59.

[29] Lessene G, Czabotar PE, Colman PM. BCL-2 family antagonists for cancer therapy. Nat Rev Drug Discov 2008;7:989–1000.
[30] Cimmino A, Calin GA, Fabbri M, Iorio MV, Ferracin M, Shimizu M, et al. MiR-15 and miR-16 induce apoptosis by targeting BCL2. Proc Natl Acad Sci USA 2005;102:13944–13949.
[31] Mott JL, Kobayashi S, Bronk SF, Gores GJ. Mir-29 regulates Mcl-1 protein expression and apoptosis. Oncogene 2007;26:6133–6140.
[32] Lagos-Quintana M, Rauhut R, Lendeckel W, Tuschl T. Identification of novel genes coding for small expressed RNAs. Science 2001;294:853–858.
[33] Takamizawa J, Konishi H, Yanagisawa K, Tomida S, Osada H, Endoh H, et al. Reduced expression of the let-7 microRNAs in human lung cancers in association with shortened postoperative survival. Cancer Res 2004;64:3753–3756.
[34] Johnson SM, Grosshans H, Shingara J, Byrom M, Jarvis R, Cheng A, et al. RAS is regulated by let-7 microRNA family. Cell 2005;120:635–647.
[35] Sampson VB, Rong NH, Han J, Yang Q, Aris V, Soteropoulos P, et al. MicroRNA let-7a down-regulates MYC and reverts MYC-induced growth in Burkitt lymphoma cells. Cancer Res 2007;67:9762–9770.
[36] Lee YS, Dutta A. The tumor suppressor microRNA let-7 represses the HMGA2 oncogenes. Genes Dev 2007;21:1025–1030.
[37] Johnson CD, Esquela-Kerscher A, Stefani G, Byrom M, Kelnar K, Ovcharenko D, et al. The let-7 microRNA represses cell proliferation pathways in human cells. Cancer Res 2007;67:7713–7722.
[38] Büssing I, Slack FJ, Grosshans H. let-7 microRNAs in development, stem cells and cancer. Trend Mol Med 2008;14:400–409.

Research Article

EASL EUROPEAN ASSOCIATION FOR THE STUDY OF THE LIVER | JOURNAL OF HEPATOLOGY

Expression of CD133 confers malignant potential by regulating metalloproteinases in human hepatocellular carcinoma

Keisuke Kohga†, Tomohide Tatsumi†, Tetsuo Takehara, Hinako Tsunematsu, Satoshi Shimizu, Masashi Yamamoto, Akira Sasakawa, Takuya Miyagi, Norio Hayashi*

Department of Gastroenterology and Hepatology, Osaka University Graduate School of Medicine, Osaka 565-0871, Japan

Background & Aims: Although CD133 expression is identified as a cancer stem cell marker of hepatocellular carcinoma (HCC), the detailed characteristics of HCC cells expressing CD133 remain unclear.

Methods: We examined the malignant characteristics of CD133-expressing HCC cells.

Results: CD133-expressing cells could be detected with low frequency in 5 HCC tissues. We derived two different HCC cell lines by (1) transfection of CD133 siRNA in PLC/PRF/5 cells (CD133si-PLC/PRF/5), and (2) by a magnetic cell sorting method that allowed to divide Huh7 cells into two CD133 positive (+) and negative (−) groups. CD133 knockdown in PLC/PRF/5 cells resulted in a decrease of the mRNA and protein expressions of matrix metalloproteinase (MMP)-2 and a disintegrin and metalloproteinase (ADAM)9. We next examined the malignant characteristics related to decreasing MMP-2 and ADAM9 in HCC cells. In CD133si-PLC/PRF/5 cells and CD133− Huh7 cells, invasiveness and vascular endothelial growth factor (VEGF) production, which are both related to the activity of MMP-2, were inhibited compared to CD133-expressing HCC cells. We previously demonstrated that ADAM9 protease plays critical roles in the shedding of MHC class I-related chain A (MICA) which regulates the sensitivity of tumor cells to natural killer cells (NK). Decreasing ADAM9 expression in CD133si-PLC/PRF/5 cells and CD133− Huh7 cells resulted in an increase in membrane-bound MICA and a decrease in soluble MICA production. Both CD133si-PLC/PRF/5 cells and CD133− Huh7 cells were susceptible to NK activity, depending on the expression levels of membrane-bound MICA, but CD133-expressing HCC cells were not.

Conclusion: These results demonstrate that CD133 expression in HCC cells confers malignant potential which may contribute to the survival of HCC cells.

© 2010 European Association for the Study of the Liver. Published by Elsevier B.V. All rights reserved.

Keywords: CD133; MMP-2; ADAM9; Hepatocellular carcinoma; NK activity.
Received 18 September 2009; received in revised form 25 December 2009; accepted 30 December 2009

*Correspondence to: N. Hayashi, Department of Gastroenterology and Hepatology, Osaka University Graduate School of Medicine, 2-2 Yamadaoka, Suita, Osaka 565-0871, Japan. Tel.: +81 6 6879 3621; fax: +81 6 6879 3629.
E-mail addresses: tatsumit@gh.med.osaka-u.ac.jp (T. Tatsumi), hayashin@gh.med.osaka-u.ac.jp (N. Hayashi).
†These authors contributed equally to this work.

Abbreviations: HCC, hepatocellular carcinoma; VEGF, vascular endothelial growth factor; CSCs, cancer stem cells; MMP, matrix metalloproteinase; ADAM, a disintegrin and metalloproteinase; MICA, MHC class I-related chain A; Ab, antibody; siRNA, small interfering RNA.

Introduction

Chronic liver disease caused by hepatitis virus infection and non-alcoholic steatohepatitis leads to a predisposition for hepatocellular carcinoma (HCC) [1]. With regard to treatment, surgical resection, percutaneous techniques such as ethanol injection and radiofrequency ablation and transcatheter arterial chemoembolization (TACE) are well established and improve the prognosis of HCC patients [2]. HCC is an aggressive tumor with early vascular invasion and metastasis, and the expression of angiogenic factors such as vascular endothelial growth factor (VEGF), may help predict the prognosis of HCC patients [3]. Elucidation of the tumor biology of HCC is important to develop better ways to treat it.

The existence of cancer stem cells (CSCs) has been reported for many cancers [4], including those of the breast, brain, colon, pancreas, and blood. CSCs have been characterized in solid tumors using a variety of stem cell markers including CD133 [5]. CD133+ HCC cells isolated from human HCC cell lines and xenograft tumors possess a greater colony forming efficacy, a higher proliferative output, and a greater ability to form tumors in vivo [6–8]. Preliminary studies have demonstrated that the expression of ATP-binding cassette drug transporters is high in CD133+ cells, and that it increases the resistance of CD133+ CSCs to chemotherapeutic agents [9]. Chemo-resistant CD133+ HCC cells displayed preferential activation of the Akt/PKB and Bcl-2 pathway, promoting cell survival by suppressing apoptosis [10]. Hence, the significance of CD133 expression in cancer cell seems to be important for the development of cancer. A clearer understanding of the characteristics of CD133-expressing HCC is therefore required to establish new cancer therapies against HCC.

The metalloprotease family includes various types of proteases, such as the matrix metalloproteinases (MMPs) and a disintegrin and metalloproteinases (ADAMs), and have been reported

Cancer

to be involved in tumor-induced angiogenesis, tumor invasion, and tumor escape mechanisms from immune cells in various cancers [11,12]. Although the expression of metalloproteinase has been reported in human HCC [13], the significance of their presence in CD133-expressing cells remains unclear.

In the current study, we evaluated the malignant characteristics of CD133-expressing human HCC cells, which have a greater ability of invasion and VEGF production via MMP-2 activation. In addition, these cells were resistant to the cytolytic activity of NK cells by acting upon the ADAM9/MHC class I-related chain A (MICA) pathway. The present study shed light on the significance of CD133 expression on HCC cells and led to a new strategy for developing treatments against human HCC.

Materials and methods

HCC cell lines

Human HCC cell lines, PLC/PRF/5 cells, Huh7, HepG2, and Hep3B cells were cultured with Dulbecco's modified Eagle's medium supplemented with 10% fetal bovine serum (Gibco/Life Technologies, Grand Island, NY) in a humidified incubator at 5% CO_2 and 37 °C.

Immunohistochemistry

Five human HCC liver tissue samples (Table 1) were surgically resected after informed consent, under an Institutional Review Board-approved protocol, had been obtained. The liver sections were subjected to immunohistochemical staining by the ABC procedure (Vector Laboratories, Burlingame, CA) using the anti-CD133 antibody (Ab) (ABGENT, San Diego, CA) and the anti-CD90 Ab (AbD Serotec, Oxford, UK). The expressions of CD133 were quantified as previously described [14].

Flow cytometry

For the detection of CD133 or MICA in HCC cells, the cells were incubated with PE-conjugated anti-CD133 Ab (Miltenyl Biotech, Auburn, CA) or anti-MICA Ab (2C10, Santa Cruz Biotechnology, Santa Cruz, CA), and then subjected to flow cytometric analysis performed using a FACscan flow cytometer (Becton–Dickinson, San Jose, CA). We analyzed positive cell rates by using the control staining as previously described [15].

RNA silencing

The small interfering RNA (siRNA) method was used to knockdown CD133, MMP-2 and ADAM9 expressions of PLC/PRF/5 cells as previously described [16]. The following types of siRNA were used: CD133 knockdown PLC/PRF/5 (CD133si-PLC/PRF/5), 5′-UUUCUGUGGAUGUAACUUUCAGUGU-3′; MMP-2 knockdown PLC/PRF/5 (MMP-2si-PLC/PRF/5), 5′-UAGUGUGUCCUUCAGCACAAACAGG-3′; ADAM9 knockdown PLC/PRF/5 (ADAM9si-PLC/PRF/5), 5′-UGUCCAAACACAUUAAUCCCGCCUG-3′; control-PLC/PRF/5, negative universal control.

Table 1. Clinical background of HCC patients.

Sex	Age	Eology	Non-cancerous tissue
male	73	HCV	LC
male	67	HCV	LC
male	76	NBNC	normal
female	51	HBV	LC
female	45	HBV	LC

HBV, hepatitis B virus; HCV, hepatitis C virus; NBNC, patients without HBV and HCV; LC, liver cirrhosis.

Cell separation

CD133+/− Huh7 cells were isolated by magnetic cell sorting using CD133 MicroBeads according to the manufacturer's instructions (Miltenyl Biotech). The isolated CD133+/− Huh7 cells were injected subcutaneously into nude mice to evaluate the tumorigenicity of each cell. We found that CD133+ Huh7 cells were more tumorigenic than CD133− Huh7 cells (Fig. 1A).

Western blotting

Cells were lysed and immunoblotted as previously described [16]. For immunodetection, the following Abs were used: anti-MMP-2 Ab (Thermo Fisher Scientific, Fremont, CA) and anti-ADAM9 Ab (R&D Systems, Minneapolis, MN). To assess the protein levels, optical densities of bands in each blot were analyzed using ImageJ 1.40 g.

MMP-2 Zymography

Proteolytic activity of supernatant was examined by gelatin zymography according to the manufacturer's protocol (Cosmo-Bio, Tokyo, Japan). The supernatants of cells were subjected to 10% SDS–polyacrylamide gel electrophoresis using gels containing 0.3% gelatin. The proteolytic band of 62 kDa corresponding to the active form of MMP-2 was scanned using a Photo scanner.

Real-time RT-PCR

Total RNA extraction and reverse transcription were performed as previously described [16]. Ready-to-use assays (Applied Biosystems, Foster city, CA) were used for the quantification of MMP-2,9,14, ADAM8,9,10,12,17, TIMP-1,2,3, MICA, and β-actin according to the manufacturer's instructions. The thermal cycling conditions for all genes were 2 min at 50 °C and 10 min at 95 °C, followed by 40 cycles at 95 °C for 15 s and 60 °C for 1 min. β-Actin mRNA from each sample was quantified as an endogenous control of internal RNA.

Invasion assays

The invasion activity was measured by Boyden-chamber assay using BD BioCoat Matrigel Invasion Chamber (BD Biosciences) as previously described [17]. To assess the involvement of MMP-2 protein in the invasion activity, active-form MMP-2 proteins (20 μM, R&D systems) were added to the culture of CD133si-PLC/PRF/5 cells or CD133− Huh7 cells.

ELISA

HCC cells were cultured for 24 h and the supernatants were subjected to enzyme-linked immunosorbent assay (ELISA). Concentrations of VEGF and soluble MICA were evaluated by QuantiGlo human VEGF Immunoassay (R&D Systems) and by the DuoSet MICA eELISA kits (R&D Systems) according to the manufacturer's recommendations.

WST-8 assay

Cell growth of CD133si-PLC/PRF/5 or control-PLC/PRF/5 cells was determined by WST-8 assay (Nacalai tesque, Kyoto, Japan) as previously described [16].

NK cell analysis

NK cells were isolated from peripheral blood mononuclear cells by magnetic cell sorting using CD56 MicroBeads according to the manufacturer's instructions (Miltenyl Biotech). More than 95% of the cells were $CD56^+CD3^-$ lymphocytes. The cytolytic ability of NK cells was assessed by 4-h ^{51}Cr-releasing assay with or without MICA/B-blocking Ab (R&D systems).

Statistics

All values were expressed as the mean and SD. The statistical significance of differences between the groups was determined by applying Student's t test or the two-sample t test with Welch correction after each group had been tested with equal variance and Fisher's exact probability test. We defined statistical significance as $p < 0.05$.

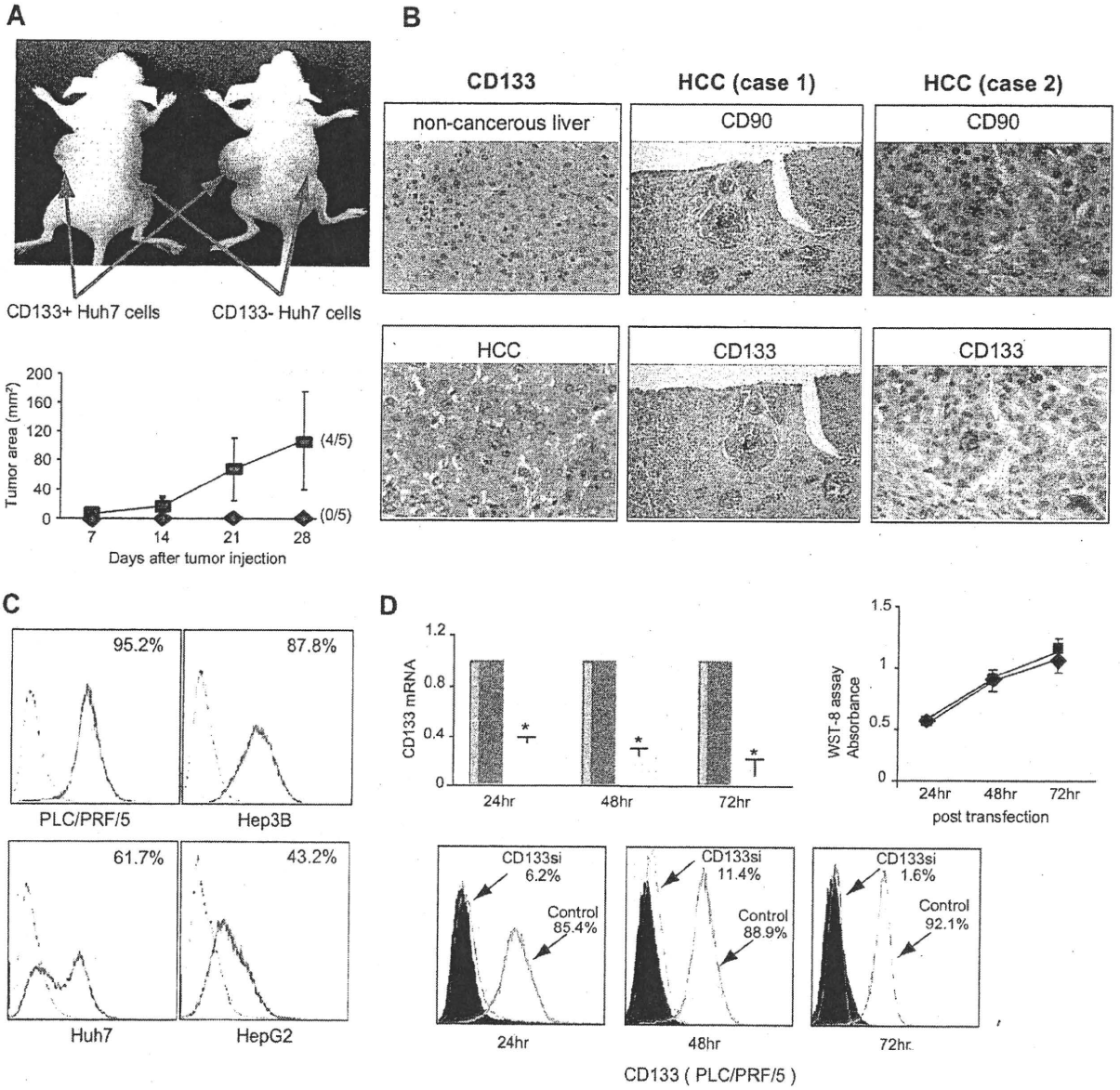

Fig. 1. Tumorigenicity of CD133+/– Huh7 cells in nude mice and the expressions of CD133 in human HCC tissues and cell lines, and CD133 knockdown in PLC/PRF/5 cells. (A) Evaluation of the phenotypes of CD133+/– Huh7 cells in a xenograft growth model. We separated CD133+/– cells using magnetic beads and injected subcutaneously 2.5×10^6 CD133+ (■, left flank) or CD133– (♦, right flank) Huh7 cells into BALB/c nu/nu mice ($N = 5$/each group). Representative macroscopic view of each group, 28 days after tumor injection, is shown (upper panel). The tumor size was monitored every week (lower panel). The fraction of mice of each group, bearing tumor after 28 days, is given in parentheses. (B) Immunohistochemical detection of CD133 in human HCC tissues and non-cancerous liver tissues ($N = 5$). Immunohistochemical detection of CD133 and CD90 in human HCC tissues ($N = 5$). Representative images are shown. (C) Human HCC cell lines were stained with anti-CD133 Ab and subjected to flow cytometry. Black lines, control IgG staining; green lines, CD133 staining. Positive cell rates are shown in the figure. (D) PLC/PRF/5 cells were transfected with CD133 siRNA (CD133si-PLC/PRF/5) or control siRNA (control-PLC/PRF/5). The mRNA and protein expressions of CD133 were evaluated by real-time PCR (left upper panel, white bar, CD133si-PLC/PRF/5 cells; black bar, control-PLC/PRF/5 cells) and flow cytometry (lower panel). Black curves, control IgG staining; red line, CD133 staining of CD133si-PLC/PRF/5 cells; blue line, CD133 staining of control-PLC/PRF/5 cells. Positive cell rates are shown in the figure. The viability of siRNA-transfected cells was evaluated by WST-8 assay (right upper panel). CD133si-PLC/PRF/5 cells (♦) and control-PLC/PRF/5 cells (■).

Results

Detection of CD133+ cells in human HCC tissues and CD133 expressions in human HCC cell lines

We examined the presence of CD133+ cells in HCC tissues. As shown in Fig. 1B, CD133+ cells could be detected with low frequency in HCC tissues (2.2 ± 1.6%) and was undetectable in non-cancerous liver tissues (0.0%). The expression of CD90, another HCC CSC marker [18], could also be detected in CD133+ cells. Similar results were observed in all five HCC tissues. We examined CD133 expressions in four human HCC cell lines. All cells were CD133 positive in both PLC/PRF/5 and Hep3B cells, and about half of the cells were CD133 positive in Huh7 and HepG2 cells (Fig. 1C).

Expression of MMP-2 and ADAM9 in CD133si- and control-PLC/PRF/5 cells and CD133+/– Huh7 cells

We established CD133si-PLC/PRF/5 cells by transfection of CD133 siRNA (Fig. 1D). The expression of CD133 mRNA and protein in CD133si-PLC/PRF/5 cells was inhibited within 72 h after transfection. The cell viability of CD133si-PLC/PRF/5 cells was similar to that of control-PLC/PRF/5 cells within 72 h after transfection (Fig. 1D). Next, we examined the mRNA expression of MMPs, ADAMs, and TIMPs. The mRNA expression of MMP-2 and ADAM9 in CD133si-PLC/PRF/5 cells was significantly lower than in control-PLC/PRF/5 cells (Fig. 2A and B); however, the expression of other metalloproteinases such as MMP-9,14, ADAM8,10,12,17, and TIMP-1,2,3 was not affected (data not shown). The protein (pro-form and active form) expressions of both MMP-2 and ADAM9 decreased in CD133si-PLC/PRF/5 cells compared to control-PLC/PRF/5 cells (Fig. 2A and B). A protein zymography assay for MMP-2 was consistent with this result in that the activity of MMP-2 protein in CD133si-PLC/PRF/5 cells also decreased compared to control-PLC/PRF/5 cells (Fig. 2A).

In Huh7 cells CD133 expression was positive in half of the cell population, as shown in Fig. 1B. We separated the Huh7 cells into CD133+ and – cells by magnetic cell sorting (Fig. 2C). The mRNA of MMP-2 in CD133– Huh7 cells was significantly lower than that of CD133+ Huh7 cells (Fig. 2C). The proteins (pro-form and active form) expressions of both MMP-2 and ADAM9 decreased in CD133– Huh7 cells as compared to CD133+ Huh7 cells (Fig. 2C and D).

The invasion ability of CD133si- and control-PLC/PRF/5 cells, and CD133+/– Huh7 cells

Human HCC cells require MMP-2 activity for invasion [19]. The invasion of PLC/PRF/5 cells transfected for siRNA against MMP-2 (MMP-2si-PLC/PRF/5 cells) was significantly lower than that of control cells (Fig. 3A). Of note, is the finding that the invasion of CD133si-PLC/PRF/5 cells was significantly lower than that of control cells (Fig. 3B). In order to examine the involvement of MMP-2 protein in the invasion activity, MMP-2 protein was added to the culture of CD133si-PLC/PRF5 cells. Although there was a tendency for MMP-2 to promote the invasion ability of CD133si-PLC/PRF/5 cells, this effect was not statistically significant (Fig. 3B).

In Huh7 cells, the invasion of CD133– Huh7 cells was significantly lower than that of CD133+ Huh7 cells (Fig. 3C). The

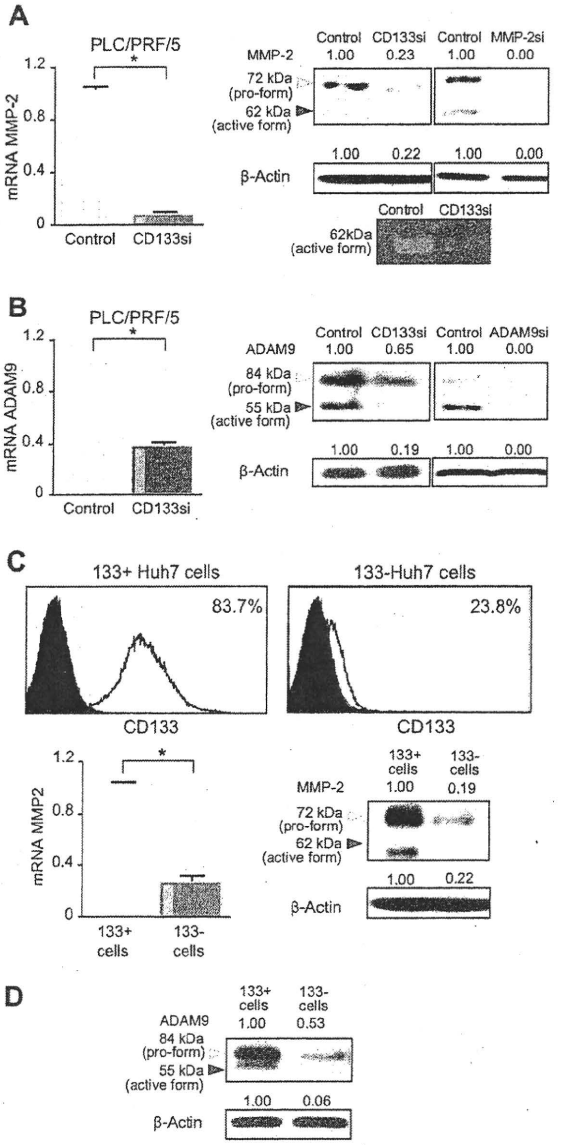

Fig. 2. Expression levels of MMP-2 and ADAM9 in CD133si-PLC/PRF/5, control-PLC/PRF/5 cells, and CD133+/–Huh7 cells. (A and C) MMP-2 mRNA and protein levels were detected by real-time PCR and Western blotting respectively, and the activity of MMP-2 was assayed by protein zymography in CD133si PLC/PRF/5si cells or control-PLC/PRF/5 cells, and CD133+/– Huh7 cells. To confirm the specificity of the anti-MMP-2 antibody used in Western blotting, the expression of MMP-2 (pro-form 72 kDa, active form 62 kDa) was evaluated in MMP-2si-PLC/PRF/5 and control-PLC/PRF/5 cells (Fig. 2A, right). (B and D) ADAM9 mRNA and protein levels, in CD133si-PLC/PRF/5 cells or control-PLC/PRF/5 cells, and CD133+/–Huh7 cells, were analyzed by real-time PCR and Western blotting respectively. To confirm the specificity of the anti-ADAM9 antibody used in Western blotting, the expression of ADAM9 (pro-form 84 kDa, active form 55 kDa) was analyzed in ADAM9si-PLC/PRF/5 and control-PLC/PRF/5 cells (Fig. 2B, right). (C) Huh7 cells were separated into CD133+ and – cells by magnetic cell sorting and the expression levels of CD133 were detected by flow cytometry. White curves, CD133 staining; black curves, control IgG staining. Positive cell rates are shown in the figure. Representative flow cytometry data are shown. Similar results were obtained from three independent experiments. Western blotting data were obtained from three independent experiments. Representative data are shown. The ratios of the protein levels (pro-form, upper side; active form, lower side) compared to control (1.00) are shown. $p < 0.05$.

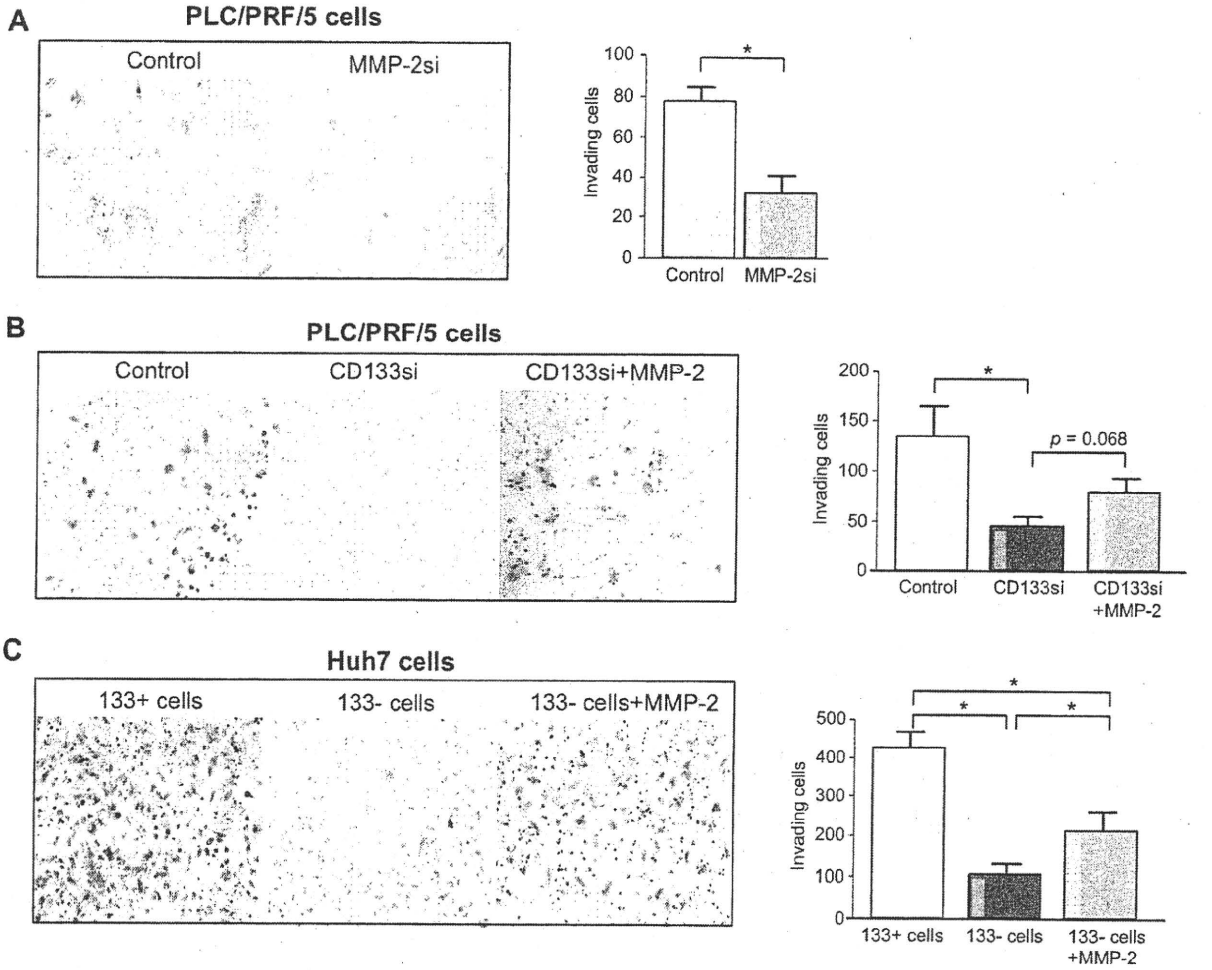

Fig. 3. The capability of invasion of CD133si-PLC/PRF5 cells, control-PLC/PRF/5 cells, and CD133+/–Huh7 cells. (A) The invasion activity of MMP-2si-PLC/PRF/5 cells or control-PLCPRF/5 cells was assayed by Boyden-chamber assay. Representative data of invading cells are shown on the left, and the quantification of the number of invading cells is shown on the right. (B) The invasion activity of CD133si-PLC/PRF/5 cells or control-PLCPRF/5 cells was evaluated by Boyden-chamber assay. Representative data of invading cells are shown on the left and the quantification of the number of invading cells is shown on the right. To assess the involvement of MMP-2 protein in the invasion activity, MMP-2 protein (20 μM) was added to CD133si-PLC/PRF/5 cultured cells. (C) The invasion activity of CD133+ and – Huh7 cells was evaluated by Boyden-chamber assay. MMP-2 protein (20 μM) was added to CD133 – Huh7 cultured cells. Representative data of invading cells are shown on the left and the quantification of the number of invading cells are shown on the right. Similar results were obtained from two independent experiments. $^{*}p < 0.05$.

MMP-2 protein was also added to the culture of CD133– Huh7 cells and this led to a significant increase in the invasiveness of CD133– cells (Fig. 3C). These results demonstrated that CD133-expressing HCC cells had higher abilities of invasion, and MMP-2 could promote the invasiveness of CD133 negative HCC cells.

The VEGF production ability of CD133si- and control-PLC/PRF/5 cells, and CD133+/– Huh7 cells

It has previously been reported that MMP-2 is associated with an increased bioavailability of VEGF [20]. In agreement with this, we observed that in MMP-2si-PLC/PRF/5 cells, the levels of VEGF were significantly lower than in control-PLC/PRF/5 cells (Fig. 4A). We then investigated the production of VEGF in CD133si- and control-PLC/PRF/5 cells, as well as in CD133– Huh7 cells. The VEGF levels of CD133si-PLC/PRF/5 cells were significantly lower than in control-PLC/PRF/5 cells (Fig. 4B), and in CD133– Huh7 cells, the VEGF levels were significantly lower than in CD133+ Huh7 cells (Fig. 4C). To examine the involvement of MMP-2 in the production of VEGF, MMP-2 was added to the culture of CD133– Huh7 cells. This led to a significant increase in the VEGF production of CD133– Huh7 cells (Fig. 4C). These results demonstrated that CD133-expressing HCC cells had an increased ability of angiogenesis because of higher expression levels of MMP-2.

CD133 knockdown resulted in increasing membrane-bound MICA expression, decreasing soluble MICA, and enhancing the cytolytic activity of NK cells in PLC/PRF/5 cells

MICA, a ligand of human NKG2D receptor, is frequently expressed in HCC and determines its sensitivity to NK cells

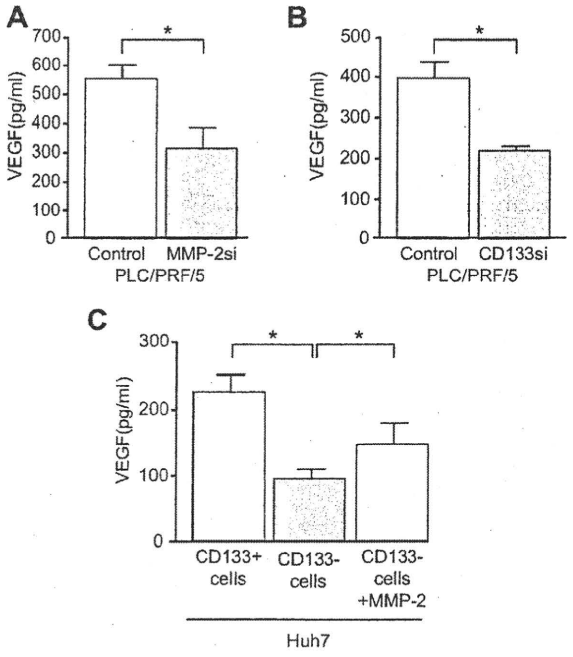

Fig. 4. Analysis of VEGF expression in CD133si-PLC/PRF/5 cells, control-PLC/PRF/5 cells, and CD133+/–Huh7 cells. (A) We measured the VEGF expression in PLC/PRF/5 cells, in presence or absence of MMP-2 protein. MMP-2si-PLC/PRF/5 or control-PLC/PRF/5 cells were cultured for 24 h and the supernatants were subjected to VEGF ELISA. (B) We next assayed the expression of VEGF in CD133si-PLC/PRF/5 cells or control-PLC/PRF/5 cells. These cells were cultured for 24 h and the supernatants were subjected to VEGF ELISA. (C) CD133+/– Huh7 cells were cultured for 24 h and the supernatants were subjected to VEGF ELISA. 133+ cells, CD133+ Huh7 cells; 133– cells, CD133– Huh7 cells; 133– cells+ MMP-2, CD133– Huh7 cells were cultured with MMP-2 protein (25 μM). Similar results were obtained from two independent experiments. $p < 0.05$.

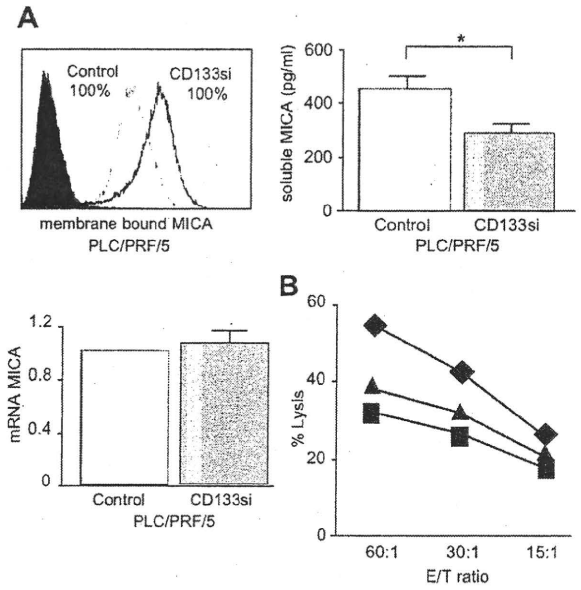

Fig. 5. Expression levels of MICA, soluble MICA production, and NK sensitivity in CD133si-PLC/PRF/5 cells and control-PLC/PRF/5 cells. (A) Expression levels of membrane-bound MICA (upper left panel) and soluble MICA production (upper right panel) in CD133si-PLC/PRF/5 cells or control-PLC/PRF/5 cells were evaluated by flow cytometry and specific ELISA respectively. Positive cell rates are shown in the figure. mRNA levels of MICA in CD133si-PLC/PRF5 or control-PLC/PRF/5 cells detected by real-time RT-PCR (lower panel). (B) We examined the cytolytic activity of NK cells against CD133si-PLC/PRF/5 cells or control-PLC/PRF/5 cells. CD133si-PLC/PRF/5 cells or control-PLC/PRF/5 cells were subjected to ^{51}Cr-release assay against NK cells. Cytolytic activity of NK cells against control-PLC/PRF/5 cells (■) or CD133si-PLC/PRF/5 cells without (♦) or with blocking antibody of MICA (▲). Similar results were obtained from two independent experiments. $p < 0.05$.

[21]. However, MICA is also proteolytically cleaved from HCC, which is an important mechanism for tumor evasion from host immunity [22]. We previously found that ADAM9 protease plays essential roles in the shedding of MICA from HCC cells [23]. The expression of membrane-bound MICA in CD133si-PLC/PRF5 cells increased, and soluble MICA production from CD133si-PLC/PRF/5 cells significantly decreased compared to the control-PLC/PRF/5 cells (Fig. 5A). In contrast, mRNA levels of MICA were equal in both CD133si-PLC/PRF/5 cells and control-PLC/PRF/5 cells (Fig. 5A). These results suggested that CD133 knockdown induced inhibition of MICA shedding in PLC/PRF/5 cells. We next evaluated the NK sensitivity of CD133si-PLC/PRF/5 cells or control-PLC/PRF/5 cells by ^{51}Cr-release assay. The cytolytic activity of NK cells against CD133si-PLC/PRF/5 cells was higher than against control-PLC/PRF/5 cells (Fig. 5B). The blocking MICA/NKG2D signal resulted in a decrease in the cytolytic activity of NK cells against CD133si-PLC/PRF/5 cells to the levels of the control-PLC/PRF/5 cells (Fig. 5B). These results were similarly observed in CD133 knockdown Hep3B and HepG2 cells (data not shown). These results suggested that control-HCC cells were more resistant than CD133 knockdown HCC cells to the cytolytic activity of NK cells due to MICA/NKG2D signals.

The expressions of membrane-bound MICA and the production of soluble MICA of CD133+/– Huh7 cells and the cytolytic activity of NK cells against CD133+/– Huh7 cells

We examined whether CD133+/– Huh7 cells exhibited similar characteristics as those observed in CD133si-PLC/PRF/5 and control-PLC/PRF/5 cells. The expression of membrane-bound MICA in CD133– Huh7 cells tended to be higher than in CD133+ Huh7 cells, and soluble MICA production from CD133– Huh7 cells was significantly lower than in CD133+ Huh7 cells (Fig. 6A). We examined the NK sensitivity of CD133+ or – Huh7 cells. The cytolytic activity of NK cells against CD133+ Huh7 cells was lower than that against CD133– Huh7 cells (Fig. 6B), as observed for CD133si- and control-PLC/PRF/5 cells.

Discussion

In order to establish new cancer therapy against HCC, the significance of CD133 expression on HCC cells needs to be elucidated. We demonstrated that CD133+ cells were observed only in HCC tissues and not in non-cancerous liver tissues, which is consistent with previous reports [8,14]. Although, all four HCC cell lines tested expressed CD133, some variations in expression was observed between cell lines; this may reflect the differences in the ability of CSCs to differentiate into progeny cells.

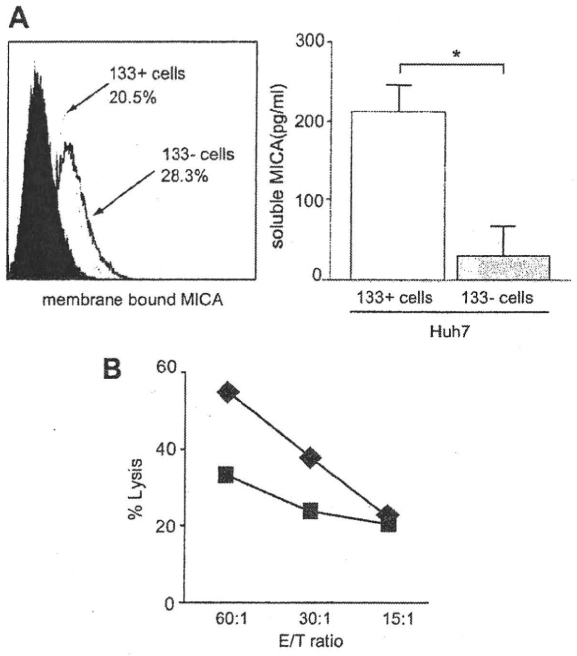

Fig. 6. Expression levels of MICA, soluble MICA production, and NK sensitivity in CD133+/− Huh7 cells. (A) Expression level of membrane-bound MICA (left panel) and soluble MICA production (right panel) in CD133+/− Huh7 cells were evaluated by flow cytometry and specific ELISA, respectively. Positive cell rates are shown in the figure. (B) We examined the cytolytic activity of NK cells against CD133+/− Huh7 cells. CD133+/− Huh7 cells were subjected to ^{51}Cr-release assay against NK cells. Cytolytic activity of NK cells against CD133+ Huh7 cells (■) or CD133− cells (♦). Representative results are shown. Similar results were obtained from two independent experiments. $p < 0.05$.

Song et al. reported that HCC patients with increased CD133 expressions in HCC tissues had shorter overall survival and higher recurrence rates compared to patients with low CD133 expression [14]. These results suggested that CD133 may have oncogenic roles in human HCC, which led us to investigate the molecular characteristics of CD133-expressing HCC cells.

We found that MMP-2 expression at mRNA and protein levels and MMP-2 activity in CD133si-PLC/PRF/5 cells decreased. This agrees with findings for CD133+/− Huh7 cells which could be divided into two groups by the expression of CD133. At present, there has been no report on the detailed relationship between the expression of CD133 molecules and MMP-2. Other MMPs (MMP-1,3,7,9,10,12,13) have an activator protein-1 (AP-1) binding site in the proximal promoter [11], while MMP-2 does not. Dai et al. demonstrated that FoxM1 directly binds to the MMP-2 promoter and regulates MMP-2 expression in glioma cells [24]. Although the detailed mechanism of inhibition of MMP-2 in CD133 negative HCC cells remains unclear, newly identified transcriptional factors may contribute to this mechanism.

A previous study demonstrated that MMP-2 knockdown mice exhibited reduced angiogenesis and impaired tumor growth [25]. CD133 knockdown resulted in the inhibition of MMP-2 activity in PLC/PRF/5 cells and the invasive ability of CD133si-PLC/PRF/5 cells was significantly impaired. These results thus suggested that the decreased activity of MMP-2 impaired the invasive ability of HCC cells. MMP-2si-PLC/PRF/5 cells also lost this ability, which supports the essential role of MMP-2 in the invasion by PLC/PRF/5 cells.

MMP-2 activity is also associated with an increased bioavailability of VEGF [20] – this latter being an important factor in the process of angiogenesis. The production of VEGF in CD133si-PLC/PRF/5 cells significantly decreased compared to that in control-PLC/PRF/5 cells, suggesting that the existence of CD133-expressing HCC cells might offer circumstances conducive to HCC survival by angiogenesis. These results were also consistent with findings for CD133+/− Huh7 cells. If the phenotype of the CD133− Huh7 cells could be reversed by transfection of the CD133 gene in CD133− Huh7 cells, this would be an evidence for the direct implication of CD133. However, transfection into CD133− Huh7 cells is technically very difficult because the reagent of transfection was toxic to CD133− Huh7 cells isolated by magnetic cell sorting. Our present results suggested that CD133 expression in HCC cells may reflect the malignant potential of HCC cells which, in turn, may influence the clinical outcomes of HCC patients.

MICA shedding is thought to be the principle mechanism by which tumor cells escape from NKG2D-mediated immunosurveillance [26]. We previously found that both ADAM9 and ADAM10 proteases were cooperatively associated with the shedding of MICA in human HCC [16,23]. Thus, it would be interesting to examine the activity of ADAMs protease in CD133-expressing HCC cells to understand how HCC tumor cells escape from innate immunity. In the present study, we demonstrated that CD133 knockdown in PLC/PRF/5 cells resulted in the decrease of ADAM9 mRNA and protein, but not of ADAM10, and was associated with the increase in expression of membrane-bound MICA as well as the decrease in production of soluble MICA in human HCC. The mRNA expression of MICA did not change between CD133si-PLC/PRF/5 cells and control-PLC/PRF/5 cells, suggesting that decreasing ADAM9 activity played an essential role in regulating MICA in CD133-expressing cells. At present, the detailed association between CD133 molecule and ADAMs proteases remains unclear. However, CD133-expressing HCC cells may be escaping from NKG2D-mediated immunosurveillance by promoting MICA shedding via ADAM9 protease.

Consistent with the results of the expressions of MICA in CD133-expressing cells, CD133 positive HCC cells are resistant and CD133 negative HCC cells are susceptible to the cytolytic activity of NK cells. Cai et al. demonstrated that the number of $CD56^+$ NK cells was reduced in HCC tissues compared to healthy donors, and $CD56^+$ NK cells in HCC patients displayed impairments in cytotoxicity and IFN-γ production [27]. This suggests that the immunological microenvironment in HCC tissues may be favorable to the survival of HCC cells, especially of CD133+ HCC cells. The specific targeting and eradication of CSCs is the most important challenge for cancer treatment. We previously demonstrated that some anti-HCC chemotherapy drugs regulated the ADAM family proteins, resulting in the enhancement of NK sensitivity [16,23]. Thus, by controlling the expression of CD133 and/or ADAM9 protease with new reagents, it may be possible to develop a new therapeutic strategy against CD133-expressing CSCs.

In spite of recent progress and early successes reported for HCC treatment, there is significant room for improvement. In

the present study, we demonstrated that CD133-expressing HCC cells have a higher ability for invasion and for producing the angiogenetic factor VEGF, and they are resistant to NK activity. These findings suggest that CD133 expression in HCC cells confers malignant potential in human HCC that may induce the growth and metastasis of HCC cells. We believe that understanding the detailed characteristics of CD133-expressing cells will pave the road for the development of new treatments for human HCC.

Conflicts of interest

The Authors who have taken part in this study declared that they do not have anything to disclose regarding funding or conflict of interest with respect to this manuscript.

Acknowledgements

This work was supported by a Grant-in-Aid from the Ministry of Education, Culture, Sports, Science and Technology of Japan and a Grant-in-Aid for Research on Hepatitis and BSE from the Ministry of Health, Labour and Welfare of Japan.
There is no financial disclosure.

References

[1] Fattovich G, Stroffolini T, Zagni I, Donato F. Hepatocellular carcinoma in cirrhosis: incidence and trends. Gastroenterology 2004;127:S35–S50.
[2] Takayasu K, Arii S, Ikai I, Omata M, Okita K, Ichida T, et al. Prospective cohort study of transarterial chemoembolization for unresectable hepatocellular carcinoma in 8510 patients. Gastroenterology 2006;131:461–469.
[3] Pang RW, Joh JW, Johnson PJ, Monden M, Pawlik TM, Poon RT. Biology of hepatocellular carcinoma. Ann Surg Oncol 2008;15:962–971.
[4] Cho RW, Clarke MF. Recent advances in cancer stem cells. Curr Opin Genet Dev 2008;18:48–53.
[5] Tang C, Ang BT, Pervaiz S. Cancer stem cell: target for anti-cancer therapy. FASEB J 2007;21:3777–3785.
[6] Suetsugu A, Nagaki M, Aoki H, Motohashi T, Kunisada T, Moriwaki H. Characterization of CD133+ hepatocellular carcinoma cells as cancer stem/progenitor cells. Biochem Biophys Res Commun 2006;351:820–824.
[7] Yin S, Li J, Hu C, Chen X, Yao M, Yan M, et al. CD133 positive hepatocellular carcinoma cells possess high capacity for tumorigenicity. Int J Cancer 2007;120:1436–1442.
[8] Ma S, Chan KW, Hu L, Lee TK, Wo JY, Ng IO, et al. Identification and characterization of tumorigenic liver cancer stem/progenitor cells. Gastroenterology 2007;132:2542–2556.
[9] Dean M, Fojo T, Bates S. Tumor stem cells and drug resistance. Nat Rev Cancer 2005;5:275–284.
[10] Ma S, Lee K, Zheng BJ, Chan KW, Guan XI. CD133+ HCC cancer stem cells confer chemoresistance by preferential expression of the Akt/PKB survival pathway. Oncogene 2008;27:1749–1758.
[11] Vihinen P, Kahari VM. Matrix metalloproteinases in cancer: prognostic markers and therapeutic targets. Int J Cancer 2002;99:157–166.
[12] Waldhauer I, Goehlsdorf D, Gieseke F, Weinschenk T, Wittenbrink M, Ludwig A, et al. Tumor-associated MICA is shed by ADAM proteases. Cancer Res 2008;68:6368–6376.
[13] Arii S, Mise M, Harada T, Furutani M, Ishigami S, Mizumoto M, et al. Overexpression of matrix metalloproteinase 9 gene in hepatocellular carcinoma with invasive potential. Hepatology 1996;24:316–322.
[14] Song W, Li H, Tao K, Li R, Song Z, Zhao F, et al. Expression and clinical significance of the stem cell marker CD133 in hepatocellular carcinoma. Int J Clin Pract 2008;62:1212–1218.
[15] Tatsumi T, Takehara T, Katayama K, Mochizuki K, Yamamoto M, Kanto T, et al. Expression of costimulatory molecules B7-1 (CD80) and B7-2 (CD86) on human hepatocellular carcinoma. Hepatology 1997;25:1108–1114.
[16] Kohga K, Takehara T, Tatsumi T, Miyagi T, Ishida H, Ohkawa K, et al. Anticancer chemotherapy inhibits MICA ectodomain shedding by downregulating ADAM10 expression in hepatocellular carcinoma. Cancer Res 2009;69:8050–8057.
[17] Yoshio T, Morita T, Kimura Y, Tsujii M, Hayashi N, Sobue K. Caldesmon suppresses cancer cell invasion by regulating podosome/invadopodium formation. FEBS Lett 2007;581:3777–3782.
[18] Yang ZF, Ho DW, Ng MN, Lau CK, Yu WC, Ngai P, et al. Significance of CD90+ cancer stem cells in human liver cancer. Cancer Cell 2008;13:153–166.
[19] Giannelli G, Bergamini C, Fransvea E, Marinosci F, Quaranta V, Antonaci S. Human hepatocellular carcinoma (HCC) require both alpha3beta1 integrin and matrix metalloproteinases activity for migration and invasion. Lab Invest 2001;81:613–627.
[20] Rundhaug JE. Matrix metalloproteinases and angiogenesis. J Cell Mol Med 2005;9:267–285.
[21] Jinushi M, Takehara T, Tatsumi T, Kanto T, Groh V, Spies T. Expression and role of MICA and MICB in human hepatocellular carcinomas and their regulation. Int J Cancer 2003;104:354–361.
[22] Jinushi M, Takehara T, Tatsumi T, Hiramatsu N, Sakamori R, Yamaguchi S, et al. Impairment of natural killer cell and dendritic cell functions by the soluble form of MHC class I-related chain A in advanced human hepatocellular carcinoma. J Hepatol 2005;43:1013–1020.
[23] Kohga K, Takehara T, Tatsumi T, Ishida H, Miyagi T, Hosui A, et al. Sorafenib inhibits the shedding of MICA on hepatocellular carcinoma cell by downregulating ADAM9. Hepatology, in press.
[24] Dai B, Kang SH, Gong W, Liu M, Aldape KD, Sawaya R, et al. Aberrant FoxM1B expression increases matrix metalloproteinase-2 transcription and enhances the invasion of glioma cells. Oncogene 2007;26:6212–6219.
[25] Itoh T, Tanioka M, Yoshida H, Yoshioka T, Nishimoto H, Itohara S. Reduced angiogenesis and tumor progression in gelatinase A-deficient mice. Cancer Res 1998;58:1048–1051.
[26] Groh V, Wu J, Yee C, Spies T. Tumor-derived soluble MIC ligands impair expression of NKG2D and T-cell activation. Nature 2002;419:734–738.
[27] Cai L, Zhang Z, Zhou L, Wang H, Fu J, Zhang S, et al. Functional impairment in circulating and intrahepatic NK cell and relative mechanism in hepatocellular carcinoma patients. Clin Immunol 2008;129:428–437.

GASTROENTEROLOGY 2010;138:2487–2498

Thrombocytopenia Exacerbates Cholestasis-Induced Liver Fibrosis in Mice

TAKAHIRO KODAMA,* TETSUO TAKEHARA,* HAYATO HIKITA,* SATOSHI SHIMIZU,* WEI LI,* TAKUYA MIYAGI,* ATSUSHI HOSUI,* TOMOHIDE TATSUMI,* HISASHI ISHIDA,* SEIJI TADOKORO,‡ AKIO IDO,§ HIROHITO TSUBOUCHI,§ and NORIO HAYASHI*

*Department of Gastroenterology and Hepatology and ‡Department of Hematology and Oncology, Osaka University Graduate School of Medicine, Suita, Osaka; and §Digestive Disease and Life-style Related Disease Health Research, Human and Environmental Science, Kagoshima University Graduate School of Medical and Dental Science, Kagoshima, Kagoshima, Japan

BACKGROUND & AIMS: Circulating platelet counts gradually decrease in parallel with progression of chronic liver disease. Thrombocytopenia is a common complication of advanced liver fibrosis and is thought to be a consequence of the destruction of circulating platelets that occurs during secondary portal hypertension or hypersplenism. It is not clear whether thrombocytopenia itself affects liver fibrosis. **METHODS:** Thrombocytopenic mice were generated by disruption of *Bcl-xL*, which regulates platelet life span, specifically in thrombocytes. Liver fibrosis was examined in thrombocytopenic mice upon bile duct ligation. Effect of platelets on hepatic stellate cells (HSCs) was investigated in vitro. **RESULTS:** Thrombocytopenic mice developed exacerbated liver fibrosis, with increased expression of type I collagen $\alpha 1$ and $\alpha 2$, during cholestasis. In vitro experiments revealed that, upon exposure to HSCs, platelets became activated, released hepatocyte growth factor (HGF), and then inhibited HSC expression of the type I collagen genes in a Met signal-dependent manner. In contrast to the wild-type mice, the thrombocytopenic mice did not accumulate hepatic platelets or phosphorylate Met in the liver following bile duct ligation. Administration of recombinant HGF to thrombocytopenic mice reduced liver fibrosis to the levels observed in wild-type mice and attenuated hepatic expression of the type I collagen genes. **CONCLUSIONS: Thrombocytopenia exacerbates liver fibrosis; platelets have a previously unrecognized, antifibrotic role in suppressing type I collagen expression via the HGF-Met signaling pathway.**

Keywords: Bcl-2; Apoptosis; Cre; Conditional Knockout.

Cirrhosis followed by chronic liver disease is considered to be a major medical issue worldwide, causing significant morbidity and mortality because it can progress to liver failure or develop into hepatocellular caricinoma. The pathogenesis of cirrhosis is characterized by liver fibrosis, which is defined as excessive production and deposition of several extracellular matrix (ECM) proteins. The accumulation of ECM proteins, as fibrotic scars, gradually distorts liver structure and increases intrahepatic resistance to blood flow, leading to portal hypertension.[1] Among the deposited ECM proteins in the cirrhotic liver, type I collagen is the most prevalent, and it is well known that activated hepatic stellate cells (HSCs) are major collagen-producing cells.[1,2] With fibrosis progression in chronic liver disease, patients often suffer from thrombocytopenia, which promotes a tendency for bleeding and can result in mortal hemorrhagic complications such as variceal bleeding.[3] Multiple factors have been proposed for the pathogenesis of thrombocytopenia in advanced liver fibrosis; they include enhanced destruction of circulating platelets in an enlarged spleen arising because of portal hypertension[4] and reduced production of thrombopoietin (TPO) in the liver.[3] In general, concomitant thrombocytopenia is considered to be a secondary phenomenon caused by liver fibrosis progression. However, whether thrombocytopenia per se affects liver fibrosis has not been thoroughly examined. In the present study, we generated a novel mouse model of severe thrombocytopenia by thrombocyte-specific knockout of Bcl-xL, a critical regulator of thrombocyte life span,[5] and found that the mice developed exacerbated liver fibrosis during bile duct ligation (BDL)-induced cholestasis because of an increase in type I collagen gene expression. In vitro study revealed that platelets negatively regulated type I collagen gene expression in activated HSCs via a pathway involving the platelet-derived hepatocyte growth factor (HGF) and its receptor, Met.

Abbreviations used in this paper: ALP, alkaline phosphatase; α-SMA, α-smooth muscle actin; BDL, bile duct ligation; BrdU, 5-bromo-2-deoxyuridine; ECM, extracellular matrix; HGF, hepatocyte growth factor; HSCs, hepatic stellate cells; MMP, matrix metalloprotease; mRNA, messenger RNA; Pf4, platelet factor 4; siRNA, small interfering RNA; T-Bil, total bilirubin; TPO, thrombopoietin; TUNEL, terminal deoxynucleotidyl transferase-mediated deoxyuridine triphosphate nick-end labeling.

© 2010 by the AGA Institute
0016-5085/$36.00
doi:10.1053/j.gastro.2010.02.054

Materials and Methods

Mice

Thrombocyte-specific Bcl-xL knockout mice (*bcl-x$^{flox/flox}$ Pf4-Cre*) were generated by mating *bcl-x$^{flox/flox}$* mice[6,7] and *Pf4-Cre* transgenic mice.[8] They were maintained in a specific pathogen-free facility and treated with humane care under approval from the Animal Care and Use Committee of Osaka University Medical School.

BDL Treatment

Wild-type (*bcl-x$^{fl/fl}$*) and knockout (*bcl-x$^{fl/fl}$ Pf4-Cre*) mice were subjected to BDL as previously reported.[9] Briefly, the common bile duct was ligated 3 times with 5-0 silk sutures and then cut between the ligatures. After 10 days, the animals were killed for the following analyses. For more detailed description of the Materials and Methods used, see the Supplementary Materials and Methods.

Results

Thrombocyte-Specific Disruption of Bcl-xL Causes Massive Thrombocytopenia

Previous research has demonstrated that traditional knockout mice lacking a single allele of the *bcl-x* gene develop mild thrombocytopenia.[5] We generated thrombocyte-specific Bcl-xL knockout mice by crossing *floxed bcl-x* mice[6,7] and *Pf4-Cre* transgenic mice.[8] After mating *bcl-x$^{flox/flox}$Pf4-Cre* mice with *bcl-x$^{flox/flox}$* mice, *bcl-x$^{flox/flox}$Pf4-Cre* mice were born at the expected Mendelian frequency and did not show any developmental abnormality. As expected, *bcl-x$^{flox/flox}$Pf4-Cre* mice showed severe thrombocytopenia without any phenotypes of other hematopoietic lineages (Figure 1*A*). Western blot analysis confirmed a substantial decrease in Bcl-xL expression in circulating platelets of *bcl-x$^{flox/flox}$Pf4-Cre* mice compared with *bcl-x$^{flox/flox}$* mice (Figure 1*B*). CD41 protein, a specific surface receptor expressed in the thrombocyte lineage,[10,11] was used as a loading control of platelets. To demonstrate the thrombocyte-lineage specificity of the Platelet factor 4 (Pf4) promotor that we used, we examined Bcl-xL protein expression in several tissues and hematopoietic cells of *bcl-x$^{flox/flox}$ Pf4-Cre* mice and *bcl-x$^{flox/flox}$* mice by Western blotting. In all of these tissues and cells, Bcl-xL protein expression was not different between the 2 groups (Figure 1*C*), indicating that the Pf4 promotor was specific to platelets and their precursors in our mice model. The physiologic liver status was not different between the 2 groups as evidenced by serum biochemistry data for alanine transaminase (ALT), total bilirubin (T-Bil), and alkaline phosphatase (ALP) (Figure 1*D*) as well as for liver histology (Figure 1*E*). In the following experiments, *bcl-x$^{flox/flox}$ Pf4-Cre* mice were crossed with *bcl-x$^{flox/flox}$* mice, and their offspring, *bcl-x$^{flox/flox}$ Pf4-Cre* mice and *bcl-x$^{flox/flox}$* mice, were used as thrombocytopenic mice and control littermates, respectively.

Thrombocytopenic Mice Display Exacerbation of Cholestasis-Induced Liver Fibrosis

To investigate the effect of thrombocytopenia on liver fibrosis, these mice were subjected to BDL, a well-established model of liver fibrosis,[9] and examined 10 days later. Cholestasis was similarly induced in both groups as evidenced by serum levels of alkaline phosphatase and T-Bil (Figure 2*A*). Both oncotic necrosis, also known as bile infarcts, and apoptosis are characteristic features of liver injury in the BDL model.[12] Although serum ALT levels were slightly lower in the thrombocytopenic mice than in the control littermates (Figure 2*A*), the area of oncotic necrosis as well as the number of terminal deoxynucleotidyl transferase-mediated deoxyuridine triphosphate nick-end labeling (TUNEL)-positive cells in the liver was not significantly different between the 2 groups (Figure 2*B*). The number of accumulating neutrophils, which are known to play a major role in liver inflammation induced by cholestasis,[12] did not differ between the 2 groups as assessed by chloroacetate esterase staining of the liver sections (Figure 2*C*). Similarly, the T lymphocyte and macrophage population in the liver did not differ between the 2 groups as determined by real-time reverse-transcription polymerase chain reaction (Supplementary Figure 1). Upon BDL treatment, compensatory regeneration occurred, but there was no significant difference between the 2 groups as determined by the count of 5-bromo-2-deoxyuridine (BrdU)-positive cells (Figure 2*D*).

To assess liver fibrosis, hepatic collagen deposition was evaluated by picrosirius red staining of liver sections. Collagen deposition increased following BDL treatment in both groups and was significantly higher in the thrombocytopenic mice than in the control littermates (Figure 2*E*). Similarly, the hepatic hydroxyproline content, a biochemical marker of collagen accumulation,[6] in the thrombocytopenic mice was elevated to a level significantly higher than in the control littermates (Figure 2*E*). The major form of collagen in cirrhosis is known to be type I collagen composed of 2 α1 and 1 α2 chains. After BDL, hepatic expression of type I collagen α1 and α2 genes, *col1a1* and *col1a2*, sharply rose in both groups and was significantly higher in the thrombocytopenic mice than in the control littermates (Figure 2*F*). Western blot analysis confirmed that the hepatic expression of type I collagen protein was higher in the thrombocytopenic mice than in the control littermates (Figure 2*F*). These results indicated that thrombocytopenia enhanced collagen synthesis in the liver and exacerbated liver fibrosis without affecting liver inflammation, apoptosis, and regeneration.

Platelets Become Activated and Inhibit Collagen Synthesis in Activated HSCs In Vitro

To explore the underlying mechanisms of increased collagen synthesis after BDL in the liver of the thrombocytopenic mice, we tested the hypothesis that

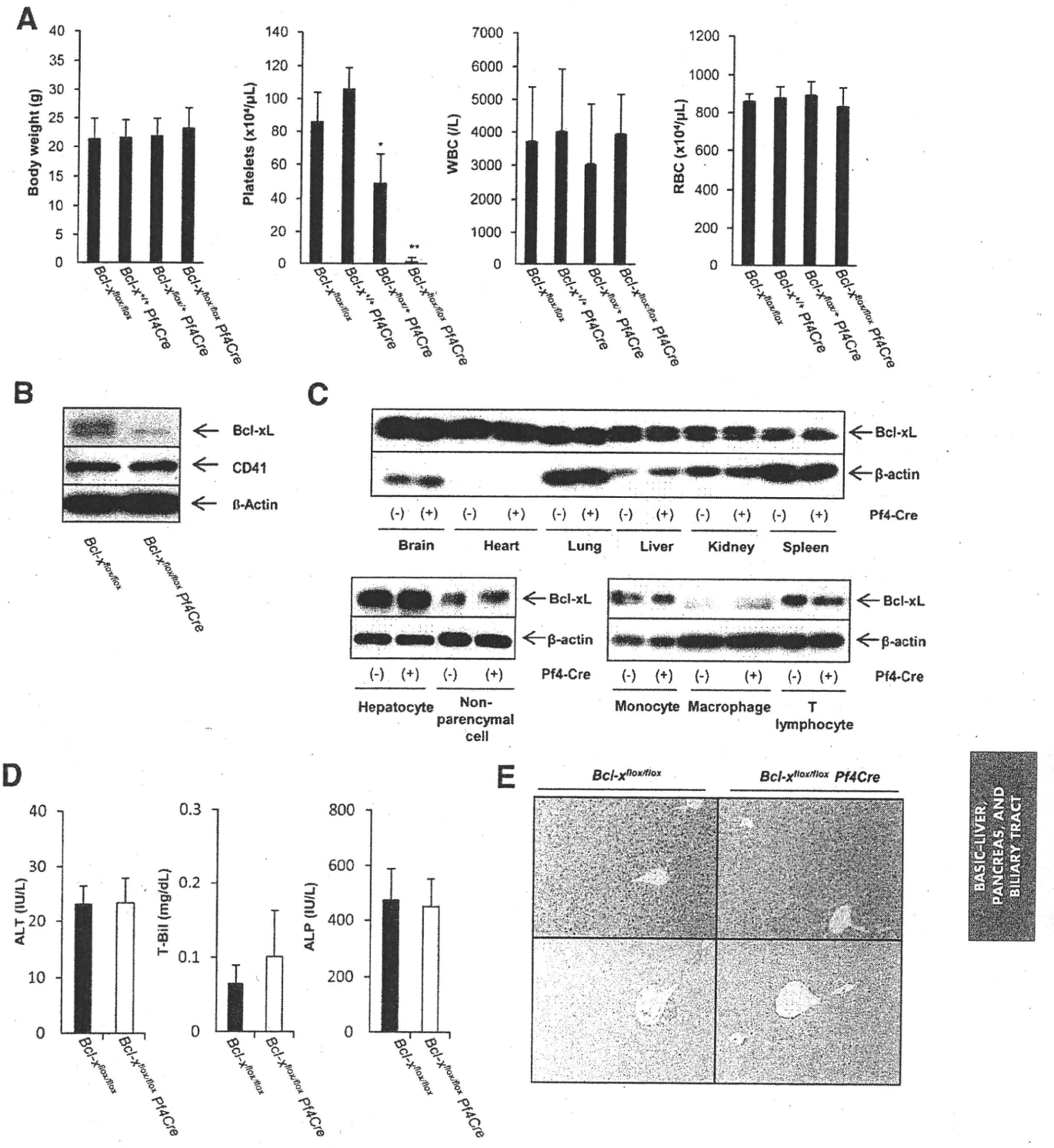

Figure 1. Thrombocyte-specific Bcl-xL knockout mice show massive thrombocytopenia. (*A*) Body weight and circulating blood cell counts of offspring from mating of *bcl-x*$^{flox/+}$ *Pf4-Cre* mice and *bcl-x*$^{flox/+}$ mice; 7–11 mice per group; **P* < .05 vs the other 3 groups, ***P* < .05 vs the other 3 groups. (*B*) Expression of Bcl-xL and CD41 protein in circulating platelets by Western blot analysis. β-Actin is included as a control. (*C*) Expression of Bcl-xL in indicated tissues and cells by Western blot analysis. Heart tissue lysates were equally loaded between the 2 groups confirmed by expression of glyceraldehyde-3-phosphate dehydrogenase, although the data are not shown. Pf4-Cre(+) and Pf4-Cre(−) stand for *bcl-x*$^{flox/flox}$ *Pf4-Cre* and *bcl-x*$^{flox/flox}$, respectively. (*D*) Serum levels of alanine aminotransferase (*ALT*), total bilirubin (*T-Bil*), and alkaline phosphatase (*ALP*). (*E*) H&E staining (*upper panel*) and picrosirius red staining (*lower panel*) of liver sections.

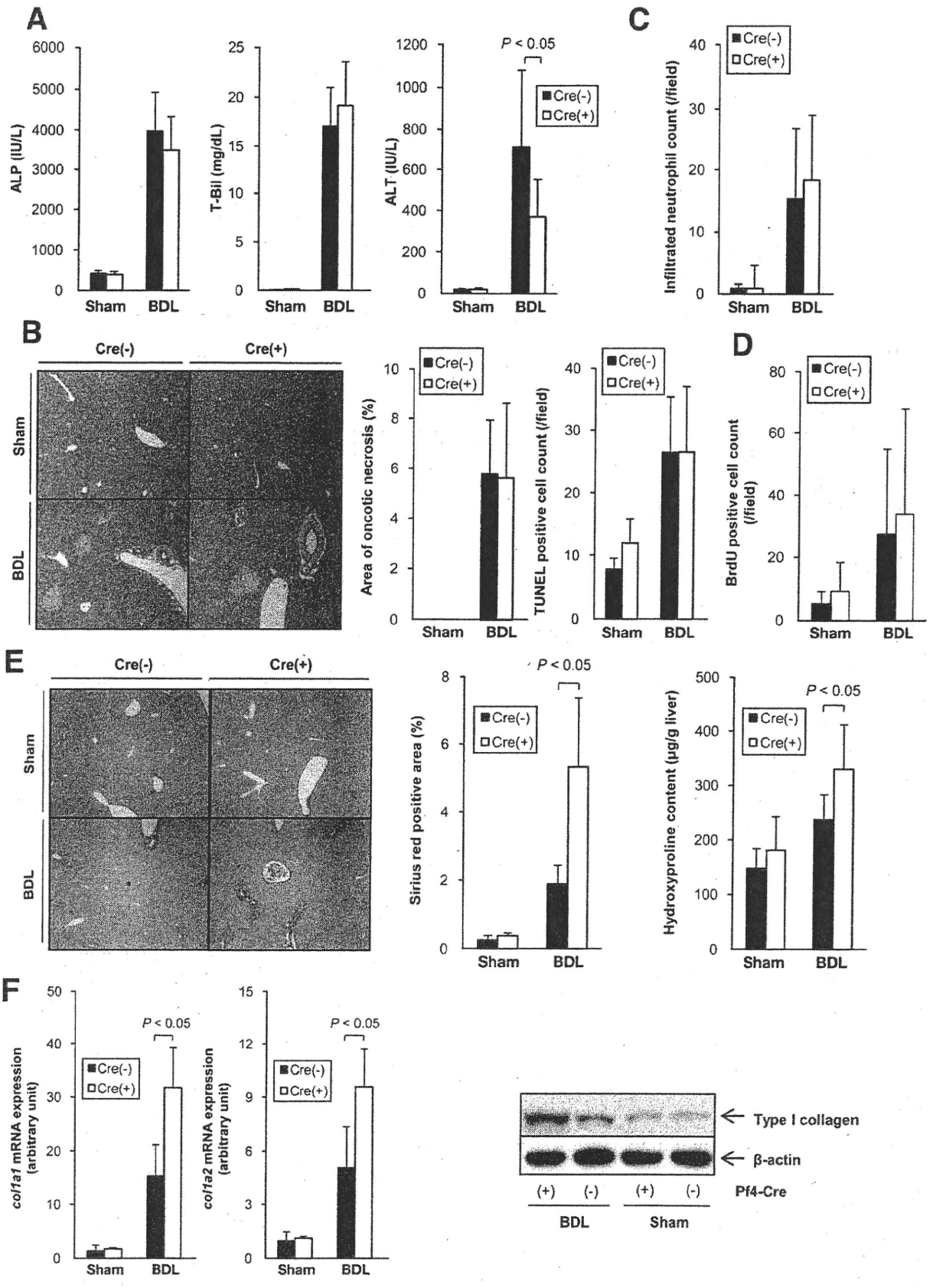
A
ALP (IU/L)
T-Bil (mg/dL)
ALT (IU/L)
P < 0.05
Cre(-)
Cre(+)
Sham
BDL
C
Infiltrated neutrophil count (/field)
B
Cre(-)
Cre(+)
Sham
BDL
Area of oncotic necrosis (%)
TUNEL positive cell count (/field)
D
BrdU positive cell count (/field)
E
Sirius red positive area (%)
Hydroxyproline content (μg/g liver)
F
col1a1 mRNA expression (arbitrary unit)
col1a2 mRNA expression (arbitrary unit)
Type I collagen
β-actin
Pf4-Cre
(+)
(-)

platelets would suppress collagen production in activated HSCs, which are known as the main collagen-producing cells in the injured liver.[13] We isolated HSCs from C57BL/6J mice and cultured them for 7 to 10 days, leading to their transdifferentiation from quiescent cells to activated myofibroblast-like cells.[13] These culture-activated HSCs were then cocultured with platelets isolated from C57BL/6J mice. Expression of *col1a1* and *col1a2* messenger RNA (mRNA) in HSCs was clearly inhibited upon addition of platelets (Figure 3*A*). After a few passages, similar suppression of type I collagen gene expression was observed in these cells, appearing in a platelet dose-dependent manner (Figure 3*B*). Type I collagen protein in HSCs also decreased upon coculture with platelets as determined by Western blot analysis (Figure 3*C*). Platelets generally execute their biologic effects through activation that is associated with their shape change and granule secretion represented by P-selectin (CD62P) translocation from the α-granule to the outer surface.[14,15] To find whether or not platelets are activated upon exposure to HSCs, platelets from cocultures with HSCs were analyzed by flow cytometry, which revealed their dynamic shape change and the surface translocation of P-selectin (Figure 3*D*). The levels of soluble P-selectin, which are also known to reflect platelet activation,[15] were significantly higher in the coculture medium with platelets and HSCs than those in the medium with platelets alone (Figure 3*E*). These results demonstrated that platelets were activated upon exposure to HSCs and inhibited collagen synthesis in activated HSCs.

Soluble Factors Released From Activated Platelets Are Involved in the Inhibition of Collagen Synthesis in HSCs

Once activated, platelets are known to affect many other cells via secreted soluble factors or direct interaction with surface molecules. Platelet activation and secretion can be triggered artificially by a variety of strong agonists such as thrombin.[14] To examine whether soluble factors secreted from activated platelets are involved in the suppression of collagen synthesis in HSCs, we stimulated platelets with or without thrombin and applied the supernatant to HSCs. Thrombin induced clear platelet activation as evidenced by shape changes and P-selectin translocation (Figure 4*A*). The levels of soluble P-selectin were also significantly higher in the supernatant of thrombin-stimulated platelets than in the supernatant of unstimulated platelets (Figure 4*B*). The supernatant of thrombin-stimulated platelets suppressed type I collagen gene expression in HSCs but that of unstimulated platelets did not (Figure 4*C*), indicating that soluble factors derived from activated platelets were involved in suppressing collagen production in HSCs.

HGF in Platelet Granules Contributes to the Inhibition of Collagen Synthesis in HSCs

To identify the platelet-derived soluble factors that contribute to the suppression of collagen synthesis in HSCs, we focused on HGF, a pleiotropic growth factor,[16,17] which is known to exist in platelets.[18] We hypothesized that, in our in vitro study, HGF may be secreted from activated platelets and inhibit collagen synthesis in HSCs. Administration of recombinant HGF to HSCs inhibited *col1a1* and *col1a2* gene expression (Figure 5*A*). Consecutively, murine platelets were capable of releasing HGF upon exposure to thrombin (Figure 5*B*). Importantly, the levels of HGF were significantly higher in the coculture supernatant of HSCs and platelets than in that of platelets alone (Figure 5*C*). We next examined whether HGF secreted from activated platelets is actually involved in suppressing collagen synthesis in HSCs. The multiple biologic activities of HGF are mediated by Met, a transmembrane tyrosine kinase receptor, which transduces the effects of HGF upon phosphorylation.[19] Western blot analysis showed that the Met protein of HSCs was phosphorylated at multiple sites after coculture with platelets (Figure 5*D*) and proteins of its downstream pathways such as Erk1/2, Akt, and stat3 were phosphorylated as well (Figure 5*D*). To assess the involvement of this activated signaling in the inhibition of collagen production in HSCs, we performed small interfering RNA (siRNA)-mediated knockdown of *met*. Transfection of *met* siRNA into HSCs resulted in a substantial decrease in Met expression (Figure 5*E*) and blunted HGF-induced suppression of type I collagen gene expression (Figure 5*F*). Under these conditions, *met* knockdown abolished platelet-induced suppression of type I collagen gene expression in HSCs (Figure 5*F*). This result clearly demonstrated that HGF/Met signaling was indispensable for platelet-mediated inhibition of the collagen synthesis in activated HSCs.

Figure 2. Thrombocytopenic mice show exacerbated liver fibrosis following BDL treatment. *bcl-x$^{flox/flox}$ Pf4-Cre* mice and *bcl-x$^{flox/flox}$* mice were sham operated or subjected to BDL and analyzed 10 days later (8–12 mice per group). Cre(+) and Cre(−) stand for *bcl-x$^{flox/flox}$ Pf4-Cre* and *bcl-x$^{flox/flox}$*, respectively. (*A*) Serum levels of alkaline phosphatase (*ALP*), total bilirubin (*T-Bil*), and alanine aminotransferase (*ALT*). (*B*) Oncotic necrosis and hepatocyte apoptosis were evaluated by H&E staining and TUNEL staining of liver sections, respectively. (*C*) Infiltrated neutrophil count was evaluated by chloroacetate esterase staining of liver sections. (*D*) Liver regeneration was evaluated by 5-bromo-2-deoxyuridine (*BrdU*) staining of liver sections. (*E*) Liver fibrosis was evaluated by picrosirius red staining of liver sections and total liver hydroxyproline levels. (*F*) *co1a1* And *col1a2* mRNA levels in the liver were determined by real-time reverse-transcription polymerase chain reaction. Expression of type I collagen protein in the liver was assessed by Western blotting.

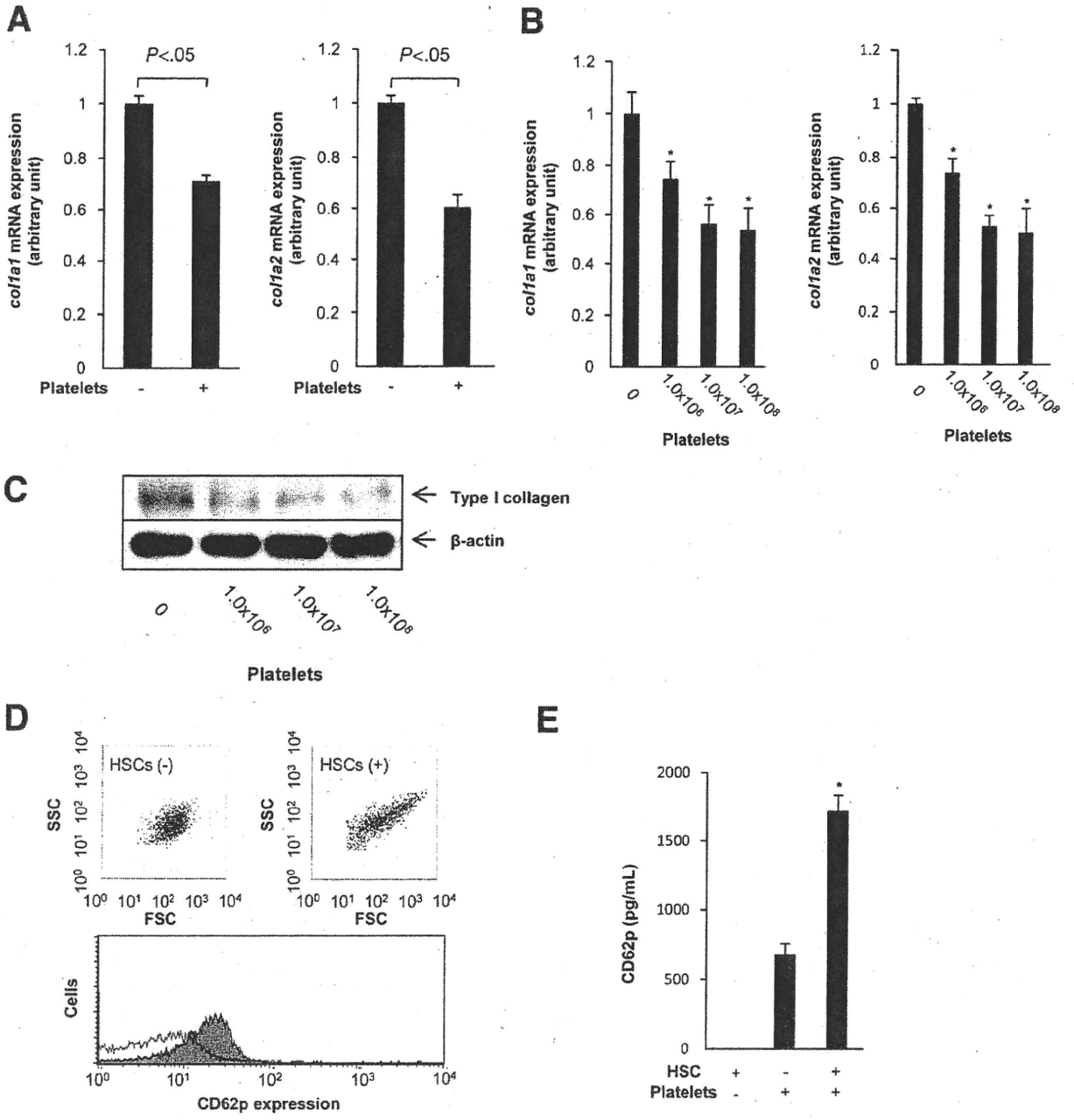

Figure 3. Platelets become activated and inhibit collagen synthesis in activated HSCs in vitro. (*A* and *B*) *co1a1* And *col1a2* mRNA levels in HSCs by real-time reverse-transcription polymerase chain reaction. Primary isolated HSCs were cocultured with 1.0×10^8 platelets for 6 hours (*A*), n = 3/group. HSCs (1.0×10^5) were cocultured with indicated dosages of platelets for 6 hours (*B*), n = 3/group, $^*P < .05$ vs HSCs with control group. (*C*) Expression of type I collagen protein in HSCs determined by Western blot analysis. HSCs (5.0×10^5) were cocultured with indicated dosages of platelets for 14 hours. (*D* and *E*) Activation of platelets on exposure to HSCs. Platelets (1.0×10^7) were cocultured with or without 1.0×10^5 HSCs for 1 hour. Shape change and P-selectin surface expression of platelets were analyzed by flow cytometry (*D*); representative data are shown; note that FSC increased with addition of HSCs; *closed histograms* and *open histograms* indicate P-selectin surface expression of platelets cocultured with or without HSCs, respectively. Soluble P-selectin levels of the culture supernatants were determined by ELISA (*E*), n = 3/group, $^*P < .05$ vs the other 2 groups.

HGF Administration Alleviates Liver Fibrosis in Thrombocytopenic Mice to the Level in the Control Littermates After BDL

To investigate the involvement of platelets in cholestasis-induced liver fibrosis in vivo, we examined platelet kinetics upon BDL treatment. To find whether platelets accumulate in the liver, we examined the expression of CD41 protein. Western blot analysis revealed that CD41 expression in the liver was up-regulated upon BDL treatment in the control littermates but not in the thrombocy-

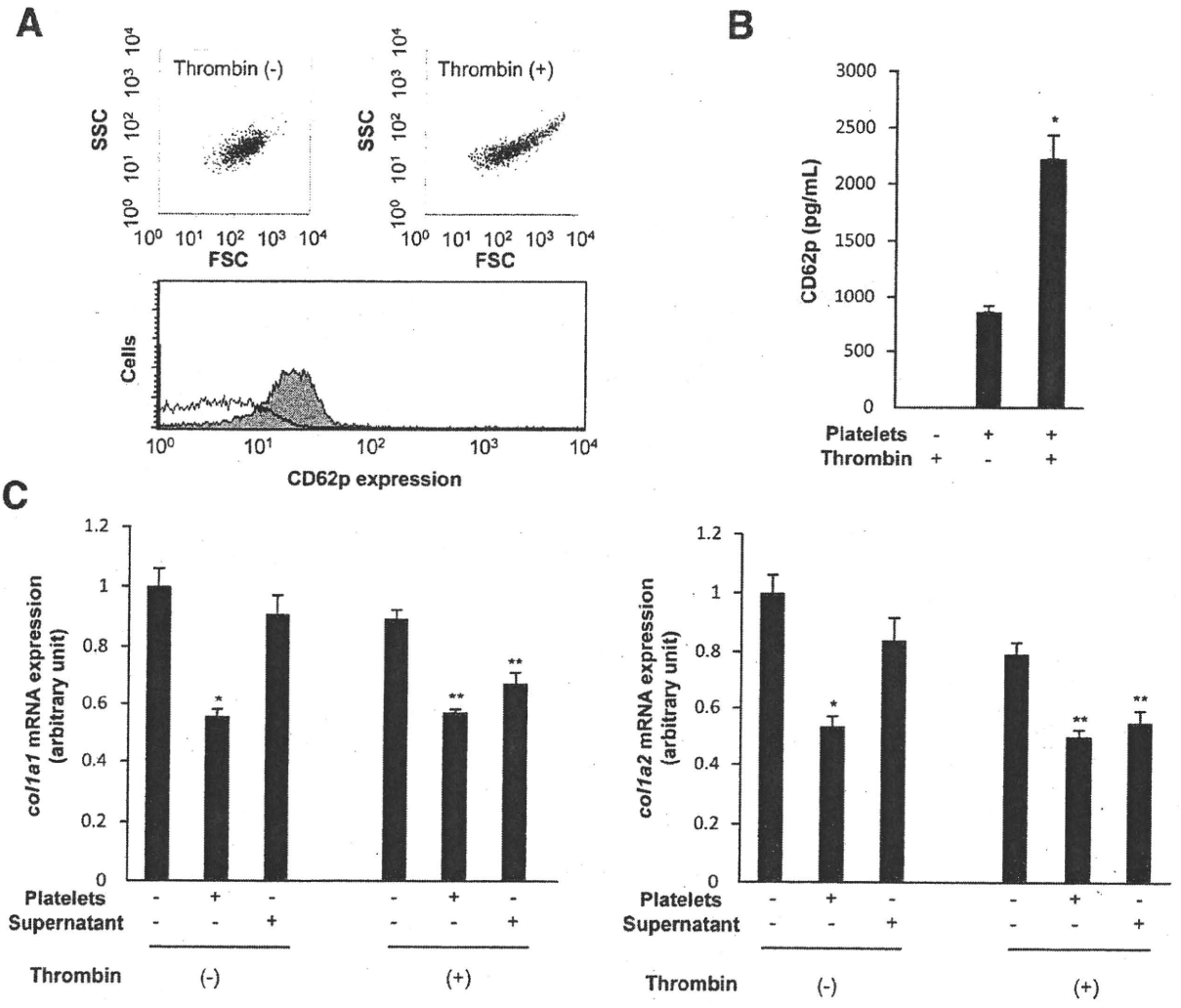

Figure 4. Soluble factors released from activated platelets are involved in the inhibition of collagen synthesis in HSCs. (*A* and *B*) Activation of platelets stimulated with thrombin. Platelets (1.0×10^7) were stimulated with or without thrombin (1 U/mL) for 15 minutes. Shape change and P-selectin surface expression of platelets were analyzed by flow cytometry (*A*); representative data are shown; note that FSC increased with addition of thrombin; *closed histograms* and *open histograms* indicate P-selectin surface expression of platelets stimulated with or without thrombin, respectively. Soluble P-selectin levels of the culture supernatants were determined by ELISA (*B*), n = 3/group, $^*P < .05$ vs the other 2 groups. (*C*) *col1a1* And *col1a2* mRNA levels in HSCs treated with the supernatant of activated or quiescent platelets by real-time reverse-transcription polymerase chain reaction. HSCs were cocultured with or without 1.0×10^7 platelets for 6 hours in the presence or absence of thrombin (1 U/mL). In parallel, HSCs were cultured for 6 hours with the supernatants of platelets, which had been stimulated with or without thrombin (1 U/mL) for 15 minutes, n = 3/group. $^*P < .05$ vs HSC with control group and HSC with platelet supernatant group. $^{**}P < .05$ vs HSC with thrombin group.

topenic mice (Figure 6*A*). Furthermore, phosphorylation of Met protein in the liver occurred upon BDL treatment, but it was weaker in the thrombocytopenic mice than in the control littermates (Figure 6*B*). Similar attenuation of Met phosphorylation in the thrombocytopenic mice was also observed at 3 days after BDL (Supplementary Figure 2). These results indicated that BDL-induced cholestasis led to intrahepatic platelet accumulation and activated the Met signal in the liver. In contrast, both were attenuated in the liver of the thrombocytopenic mice. Furthermore, plasma HGF levels in the thrombocytopenic mice did not increase upon BDL and were evidently lower than in the control littermates (Figure 6C). Finally, to investigate whether attenuation of Met activation in the liver of the thrombocytopenic mice was involved in the exacerbation of liver fibrosis, we tested the hypothesis that administration of HGF, known to exert an antifibrotic effect,[20-22] would alleviate liver fibrosis in the thrombocytopenic mice more than in the control littermates. These mice were treated with either vehicle or recombinant HGF following BDL. As expected, HGF administration alleviated liver fibrosis in the thrombocytopenic mice to the level found in the control littermates (Figure 6*D*). Notably, elevated hepatic expression of type I collagen genes in the thrombocytopenic mice was also attenuated to a level comparable with that in the control littermates by the HGF therapy (Figure 6*E*).

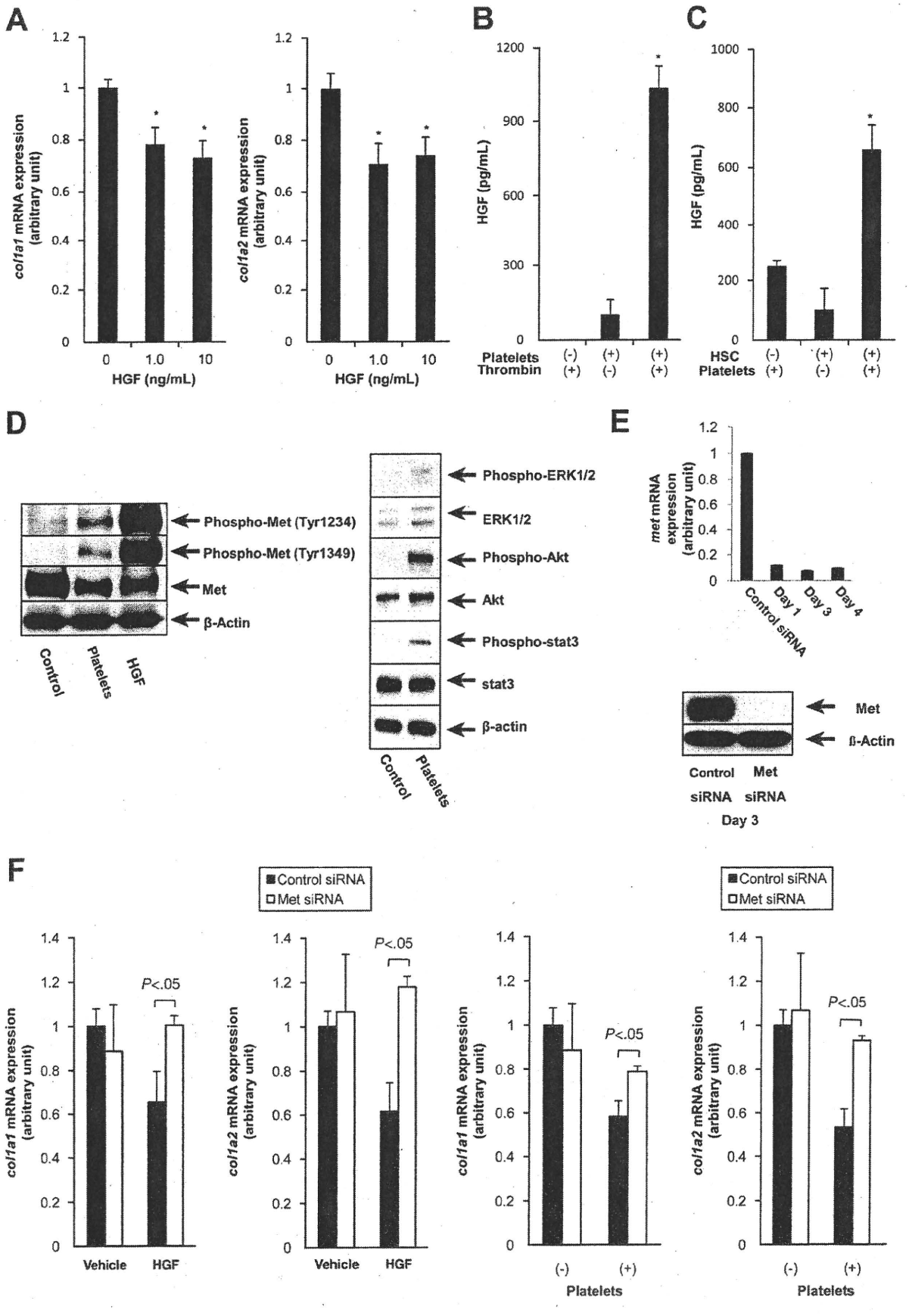
A
col1a1 mRNA expression (arbitrary unit)
HGF (ng/mL)
col1a2 mRNA expression (arbitrary unit)
HGF (ng/mL)
B
HGF (pg/mL)
Platelets
Thrombin
C
HGF (pg/mL)
HSC
Platelets
D
Phospho-Met (Tyr1234)
Phospho-Met (Tyr1349)
Met
β-Actin
Control
Platelets
HGF
Phospho-ERK1/2
ERK1/2
Phospho-Akt
Akt
Phospho-stat3
stat3
β-actin
Control
Platelets
E
met mRNA expression (arbitrary unit)
Control siRNA
Day 1
Day 3
Day 4
Met
ß-Actin
Control siRNA
Met siRNA
Day 3
F
Control siRNA
Met siRNA
col1a1 mRNA expression (arbitrary unit)
P<.05
Vehicle
HGF
col1a2 mRNA expression (arbitrary unit)
P<.05
Vehicle
HGF
col1a1 mRNA expression (arbitrary unit)
P<.05
Platelets
col1a2 mRNA expression (arbitrary unit)
P<.05
Platelets